

Review on Engineering of Bone Scaffolds Using Conventional and Additive Manufacturing Technologies" for 3D Printing and Additive Manufacturing

Mohammed, Abdullah Hanafi; Jiménez, Amaia ; Bidare, Prveen; Elshaer, Amr; Memić, Adnan; Hassanin, Hany; Essa, Khamis

License:

Other (please specify with Rights Statement)

Document Version

Peer reviewed version

Citation for published version (Harvard):

Mohammed, AH, Jiménez, A, Bidare, P, Elshaer, A, Memić, A, Hassanin, H & Essa, K 2023, 'Review on Engineering of Bone Scaffolds Using Conventional and Additive Manufacturing Technologies" for 3D Printing and Additive Manufacturing', *3D Printing and Additive Manufacturing*.

[Link to publication on Research at Birmingham portal](#)

Publisher Rights Statement:

This is an accepted manuscript version of an article accepted for publication in 3D Printing and Additive Manufacturing
<https://home.liebertpub.com/publications/3d-printing-and-additive-manufacturing/621>

General rights

Unless a licence is specified above, all rights (including copyright and moral rights) in this document are retained by the authors and/or the copyright holders. The express permission of the copyright holder must be obtained for any use of this material other than for purposes permitted by law.

- Users may freely distribute the URL that is used to identify this publication.
- Users may download and/or print one copy of the publication from the University of Birmingham research portal for the purpose of private study or non-commercial research.
- User may use extracts from the document in line with the concept of 'fair dealing' under the Copyright, Designs and Patents Act 1988 (?)
- Users may not further distribute the material nor use it for the purposes of commercial gain.

Where a licence is displayed above, please note the terms and conditions of the licence govern your use of this document.

When citing, please reference the published version.

Take down policy

While the University of Birmingham exercises care and attention in making items available there are rare occasions when an item has been uploaded in error or has been deemed to be commercially or otherwise sensitive.

If you believe that this is the case for this document, please contact UBIRA@lists.bham.ac.uk providing details and we will remove access to the work immediately and investigate.



Review on Engineering of Bone Scaffolds Using Conventional and Additive Manufacturing Technologies

Journal:	<i>3D Printing and Additive Manufacturing</i>
Manuscript ID	3DP-2022-0360.R2
Manuscript Type:	Review Papers
Date Submitted by the Author:	25-Mar-2023
Complete List of Authors:	Mohammed, Abdullah; University of Birmingham, Engineering Jiménez , Amaia; Universidad de Navarra Bidare, Prveen; University of Birmingham College of Engineering and Physical Sciences, school of mechanical engineering elshaer, Amr; Kingston University - Kingston Hill Campus memic, Adnan; King Abdulaziz University Hassanin , Hany; Canterbury Christ Church University Essa, Khamis; University of Birmingham, Mechanical Engineering
Keywords:	3D printers, additive manufacturing, hybrid additive manufacturing, medical applications
Manuscript Keywords (Search Terms):	3D printing, additive manufacturing, conventional manufacturing, bone scaffolds
Abstract:	Bone is a complex connective tissue that serves as mechanical and structural support for the human body. Bones' fractures are common, and the healing process is physiologically complex and involves both mechanical and biological aspects. Tissue engineering of bone scaffolds holds great promise for the future treatment of bone injuries. However, conventional technologies to prepare bone scaffolds can not provide the required properties of human bones. Over the past decade, three-dimensional printing or additive manufacturing technologies have enabled the control over the creation of bone scaffolds with personalized geometries, appropriate materials and tailored pores. This paper aims to review the recent advances in the fabrication of bone scaffolds for bone repair and regeneration. A detailed review of bone fracture repair and an in-depth discussion on conventional manufacturing and three-dimensional printing techniques are introduced with an emphasis on novel studies concepts, potentials and limitations.

1 **Review on Engineering of Bone Scaffolds Using Conventional and Additive** 2 **Manufacturing Technologies**

3 *Abdullah Mohammed 1, Amaia Jiménez 2, Prveen Bidare 1, Amr Elshaer 3, Adnan Memic 4,*
4 *Hany Hassanin 5, Khamis Essa 1**

5
6 1 School of Engineering, University of Birmingham, Birmingham B15 2TT

7 2 Universidad de Navarra, TECNUN Escuela de Ingeniería, Manuel de Lardizábal 15, 20018,
8 San Sebastián, Spain

9 3 Drug Discovery, Delivery and Patient Care (DDDPC), School of Life Sciences, Pharmacy
10 and Chemistry, Kingston University London, Kingston Upon Thames, Surrey, KT1 2EE, UK

11 4 Center of Nanotechnology, King Abdulaziz University, Jeddah 21589, Saudi Arabia

12 5 School of Engineering, Technology, and Design, Canterbury Christ Church University,
13 Canterbury CT1 1QU, UK

14
15 Corresponding author: Khamis Essa

16 E-mail: k.e.a.essa@bham.ac.uk

17 18 **Authorship contribution statement**

19 **Abdullah Mohammed:** Writing - Original Draft, Conceptualization, Methodology, Formal
20 analysis, Data Curation. **Amaia Jiménez:** Writing - Review & Editing. **Prveen Bidare:**

21 Writing - Review & Editing. **Amr Elshaer:** Conceptualization. **Adnan Memic:** Review

22 **Hany Hassanin:** Supervision, Project administration. **Khamis Essa:** Supervision.

23
24 **Keywords:** 3D printing, additive manufacturing, conventional manufacturing, bone scaffolds.

25 26 **Abstract**

27 Bone is a complex connective tissue that serves as mechanical and structural support for the
28 human body. Bones' fractures are common, and the healing process is physiologically
29 complex and involves both mechanical and biological aspects. Tissue engineering of bone
30 scaffolds holds great promise for the future treatment of bone injuries. However, conventional
31 technologies to prepare bone scaffolds can not provide the required properties of human
32 bones. Over the past decade, three-dimensional printing or additive manufacturing
33 technologies have enabled the control over the creation of bone scaffolds with personalized
34 geometries, appropriate materials and tailored pores. This paper aims to review the recent
35 advances in the fabrication of bone scaffolds for bone repair and regeneration. A detailed
36 review of bone fracture repair and an in-depth discussion on conventional manufacturing and

1 three-dimensional printing techniques are introduced with an emphasis on novel studies
2 concepts, potentials and limitations.

3 **1. Introduction**

4
5 Bone injuries have recently increased due to ageing, traumatic injuries, and congenital diseases,
6 making them a global health issue. It's estimated that the number of people aged more than 65
7 years will increase from 323 million to 1.55 billion by 2050 worldwide. Age intensifies the risk
8 of osteoporosis and consequently has dangerous effects on people's healthy life, disability,
9 countries' healthcare systems, and loss of productivity . Globally, over 200 million people have
10 osteoporosis, with an increased number of patients receiving hospital treatment every year due
11 to fragility fractures and bone loss, accelerating the demand for bone tissue surgeries. Efficient
12 and cost-effective strategies to treat bone injuries will help to improve people's quality of life
13 and relief the economic burden on governments (1, 2).

14 A bone defect is generally defined as the lack of bone tissue in an area of the body, which results
15 in pseudarthrosis. Usually, the human body is capable of self-repair, yet when a segmental bone
16 fracture exceeds a size of 10 mm, the body fails to self-repair (3). Therefore, external
17 interventions are essential to assist in the self-repairing process by creating bone scaffolds.
18 These scaffolds act as bridges over bone defect sites and facilitate repair (4). The design of the
19 bone substitutes must be controlled to avoid excessive bone tissue removal at defect sites and
20 to allow cell activity and proliferation (5, 6). The latter is facilitated by designing a scaffold
21 with a porous and linked pore structure. Thus, manufactured bone scaffolds are a promising
22 solution for treating bone fractures, but this comes with some challenges.

23 Regarding bone scaffolds manufacturing techniques, several methods have been investigated
24 to create porous scaffolds for bone repair, such as salt leaching, gas foaming, self-assembly,
25 phase separation, electrospinning, and freezing drying methods. Although these approaches are
26 capable of fabricating porous structures, they have certain drawbacks, such as restricted pore
27 structure control and a limited ability to customise for particular defect sites (7). Additionally,
28 many of these techniques leave behind organic residues of the pore-forming agent, impairing
29 the scaffolds' biological characteristics and lowering the quality of bone healing. Thus,
30 developing fabrications technique for scaffolds that are not restricted to obtaining the desired
31 external shape but also precisely control the pore structure is critical for their future orthopaedic
32 application.

33 Given this context, additive manufacturing (AM) technologies are becoming a good alternative
34 for manufacturing scaffolds as they can create porous scaffolds with customised external design

1 and a porous inner structure (8). The use of 3D printing technology for the generation of bone
2 scaffolds has been gaining more attention from researchers and the biomedical industry in
3 recent years. The near future of bone regeneration and healing is closely linked to developments
4 in tissue engineering. Polytherapy, which combines scaffolds, stem cells, and healing promoters
5 with new advances in tissue-engineered constructs in three-dimensional printing, may be
6 capable of overcoming current challenges in treating bone injuries. In this review paper, we will
7 focus on scaffolds as an established treatment for bone fracture using 3D printing technologies
8 and compare them with conventional manufacturing techniques (Figure 1).

9 10 **2. Bone Fracture Repair**

11 Bone tissue can undergo biological remodelling as a function of a dynamic process that involves
12 osteoclasts absorbing mature bone tissue and osteoblasts forming new bone tissue (9, 10). Bone
13 is a complex connective tissue made up of osteoblasts, osteocytes, bone lining cells, and
14 osteoclasts. The outer layers of bones are mineralised, giving them significant strength and
15 rigidity to support the body structure and allow skeletal movement. Bones composition includes
16 the inorganic phase (60% - 70% of the tissue), (22% - 35%) organic matrix and liquid (5% –
17 8%), where collagen represents the majority of the organic matrix and only 10% non-
18 collagenous proteins (11). Bones strength and stiffness are mainly provided by hydroxyapatite
19 crystal ($\text{Ca}_{10}(\text{PO}_4)_6(\text{OH})_2$) with carbonate ions (12) which are found within and between
20 collagen fibres in the form of needles, plates and rods with an average diameter of 20–80 nm
21 and 2–5 nm in thickness [2]. Bone can also modify its structure according to body requirements,
22 such as in repair, modelling, remodelling, and growth (13, 14).

23 Bone tissues can be classified into cortical and trabecular (Figure 2). Both have the same matrix
24 composition; however, they vary in structure and function as well as in relative distribution
25 between bones. Cortical bone (dense or compact) is composed of layers surrounded by lamellar
26 bone and vascular channels. This arrangement is known as the Haversian or osteon (15). An
27 osteon's central channel contains cells, vessels, nerves, and osteon-connecting Volkmann's
28 channels (15). On the other hand, trabecular bone (spongy or cancellous) is located in the
29 epiphysis and metaphysis of long bones and inside small or flat bones. Trabecular bone has a
30 wide network of individual trabeculae, small and interconnected plates and rods guided by
31 external loading (15). Typically, cortical and trabecular bones have Young's moduli of
32 approximately 17 and 1 GPa, respectively (15). Cortical bone is a dense structure representing
33 about 80% of the total skeletal tissue. Yet, cortical bones have some microscopic pores (about
34

1 10% of the total cortical bone volume) to allow vascular and neural supply and enable the
2 delivery of nutrients (16). The porosity of cortical bone is critical as an increase in intracortical
3 porosity can reduce the bone strength and consequently increase the chances of fracture (17). It
4 is evident that cortical bone becomes more fragile at very high strain levels reflecting high-
5 impact trauma (Figure 2). As the strain rate increases, cortical bone shows a ductile to brittle
6 transition (18), and like any material, the cortical bone could be prone to fatigue failure.

7 On the other hand, trabecular bone has a lower mass and high porosity when compared to
8 cortical bone. Pores represent 50%-90% of total trabecular bone volume (19). This makes it
9 considered an open cell porous foam with a reduced compressive strength to about one-tenth
10 of the cortical bone (20). It does, however, provide a large surface area that is necessary for red
11 bone marrow, blood vessels and bone-connected tissues and facilitates hematopoiesis and
12 homeostasis of minerals. The trabecular bone's physical and mechanical properties vary widely
13 depending largely on the anatomical location, age and orientation of the cell structures (21, 22).
14 Depending on the type and orientation of these basic cell structures, the mechanical properties
15 can differ by a factor of 10. A comparison between the compressive properties of trabecular
16 and cortical bones is shown in (Figure 3) (21). As shown, the cortical bone acts as a typical
17 brittle material at which the stress steeply increases at a low strain in the elastic region, and the
18 fracture occurs without a noticeable change in the strain.

19 On the other hand, trabecular undergoes a ductile behaviour under compression loading with a
20 substantial increase in the plastic deformation before fracture. Individual trabeculae bone
21 damage and repair is a physiological process that occurs throughout life and increases with age
22 (23).

23 Bone fracture healing process can be enhanced using several techniques, such as grafts, which
24 replace defected bone with another bone from the patient's own body (autografts) or from a
25 donor, or by using healing growth materials in fabricating bone implants or scaffolds (24).
26 Autografts are currently the bone regeneration golden standard (24). However, Autografts
27 techniques have several disadvantages, such as surgical complications and the limited supply
28 of natural tissue. Tissue-engineered bone scaffolds are a suitable alternative to autografts as
29 they improve fracture healing and enhance the incorporation of grafts (25, 26). Requirements of
30 tissue-engineered scaffolds are to have properties close to those of autografts irrespective of
31 their limitations (27).

1 Bone scaffolds need to have high porosity with sufficient sizes of pores across all sites of the
2 scaffold in order to create an ideal environment for the formation of new tissue matrix and bone.
3 Moreover, growth factors like the basic growth factor of fibroblasts (28, 29) can influence cell
4 functions, proliferation, or differentiation; Promotive healing agents, for example, Human
5 platelet-rich plasma (hPRP) (30-32); and also Tarantula cubensis extract (33) could be
6 incorporated into the scaffolds to improve the damaged connective tissue's ability to repair.

7 The scaffold's vascularity is important as if not present, ischemia will occur in the scaffold, and
8 hence the cells would die. Therefore, it would be useful to incorporate growth factors such as
9 FGF, PDGF, and VEGF to promote angiogenesis in scaffolds and grafts (34, 35). A
10 combination of stem cells and scaffolds with growth factors can be one possible approach
11 providing all the required characteristics to enhance bone repair and regeneration. Currently,
12 none of the grafts provided all the desirable requirements such as biocompatibility, size
13 limitation, cost, osteogenic, osteoconductive, osteoinductive, and angiogenic properties (Table
14 1). Tissue engineering seeks to provide all or most of these characteristics (36, 37). Also, tissue
15 engineering can cause bone defects to be repaired and reconstructed (27). Incorporating the
16 basics of orthopaedic surgery with knowledge from various sciences such as biology,
17 engineering, chemistry, materials science and physics could overcome current treatments'
18 shortcomings (25). Advances in biomaterials and tissue engineering can provide more
19 appropriate tools to support the differentiation and proliferation of bone cells and improve bone
20 fracture healing. Although there are a large number of studies in the literature on the effects of
21 different agents on bone healing, it is certain to investigate the best manufacturing techniques
22 for fabricating the desired scaffolds (38-40).

23

24 **3. Conventional manufacturing techniques**

25
26 Conventional techniques used to prepare bone scaffolds are based on subtractive procedures to
27 get the desired shape by removing sections of the material from an original block. The inability
28 to manage complex shapes and geometries, as well as to incorporate interior architecture,
29 cavities or curved channels, is a major disadvantage of these techniques (41). This is of special
30 importance in the biomedical industry, where complex and organic shapes are usually needed
31 for the implants to fit well. Additionally, cell viability and function can be affected by the use
32 of organic solvents, even if only residues remain (42). In order to obtain those geometries, until
33 now, several conventional manufacturing methods, such as salt leaching, gas formation, phase
34 separation, freeze-drying, electrospinning, and self-assembly, have been employed in the

1 fabrication of porous bone scaffolds despite their limitations (Figure 4). The principles of each
2 procedure are covered in the following sections. The prevalence of research on each technique
3 is summarised in (Figure 5). It is evident that more phase separation technique has attracted the
4 attention of researchers over the last 10 years.

6 3.1. Salt leaching

8 This process was widely used in the manufacture of tissue-based scaffolds. In this technique,
9 salt crystals or porogen (e.g. sodium chloride) are put in a mould, and the remaining gaps are
10 filled with a polymer. The polymer is then solidified, and salt crystals are dissolved in a suitable
11 solvent like alcohol or water by dissolution (43-45). After all the salt leaches out, a solidified
12 polymer with porosity is created, as illustrated in (Figure 4a) (46).

13 β -chitin and collagen have been successfully used to prepare using salt leaching technique. The
14 prepared membranes achieved a porosity of 77.81% and an average pore size of 260-330 μm .
15 β -chitin membranes were prepared with NaCl salt-leaching, and then collagen solution crossed
16 membranes by lyophilisation at -75°C (Figure 6a-b) shows the scaffold's cross-sectional and
17 surface morphologies. In vitro cell culture demonstrated that the human fibroblasts attached to
18 the collagen sites after 3 days, and proliferation took place within 14 days of cultivation (47).

19 The salt leaching technique enables the customisation of the pore size by adjusting the porogen
20 size employed. It is also possible to control the porosity and pore size of the scaffold by
21 manipulating the volume and size of the salt particles used, respectively (43, 48). Despite the
22 mentioned benefits of salt leaching for scaffold fabrication, this process has some limitations.
23 For instance, it is not possible to control the pore distribution or the shape of scaffolds created
24 (43). Additionally, this technique requires scaffolding to be manufactured only in the form of
25 tubes and flat sheets, which means that it is ideal for the manufacture of membrane scaffolds.
26 Besides, the use of organic solvents can negatively impact the viability of cells and their
27 biological functions (49). Although the residues of any cytotoxic solvents could be detected
28 (50), they pose limitations for general applications of salt leaching scaffolds.

30 3.2. Gas foaming

31 Gas foaming is a manufacturing approach in which a polymeric material is filled with a foaming
32 agent such as carbon dioxide, water or nitrogen at high pressure (51-53). Solid polymer disks
33

1 like polyglycolide (PGA) and poly-L-lactide (PLA) are created at high temperatures before
2 spreading high-pressure carbon dioxide gas through the disks for a few days before decreasing
3 the pressure down to the ambient level (Figure 4b) (54).

4 Gas foaming was used by Kim et al. (55) to fabricate porous biphasic calcium phosphate (BCP)
5 scaffold by using gas-foamed polyurethane as a model achieving a porosity of 75% to 85% and
6 pore size around 300-800 μm . The BCP scaffold was biocompatible and successfully
7 differentiated and regenerated bone according to both the in vivo and in vitro experiments
8 conducted in this study (55). In another study, a biodegradable poly (L-lactic acid) (PLLA)
9 scaffold with high open porosity was fabricated using a gas-foaming technique along with salt
10 leaching (56). The scaffold had a porosity of around 90% with pore sizes around 300-400 μm ,
11 which is ideal for high-density seeding of cells (Figure 7). Upon seeding rat hepatocytes into
12 the scaffold, 40% viability and around 95% seeding efficiency were achieved within 24 hours
13 (56).

14 The key advantage of using the gas foaming technique is that it does not require the use of
15 chemical solvents, thus reducing the overall manufacturing time. Nonetheless, it is challenging
16 to control the internal structure of the scaffolds in terms of pore size and high connectivity using
17 this technique (57, 58). In addition, high temperatures during the creation of disks often prevent
18 the use of bioactive molecules in scaffolds (59). Although this technique has the ability to
19 fabricate scaffolds with 93 % porosity and pore sizes up to 100 μm (59), it has been noted that
20 the scaffold interconnects only 10–30 % of the pores which may limit the proliferation of
21 encapsulated scaffold cells (54).

22 23 24 **3.3. Phase separation**

25 In phase separation, a polymer is generally dissolved in an appropriate solution and then
26 deposited in a mould that is gradually cooled till the solution freezes. The solvent is then
27 removed by freezing, leaving behind a porous matrix, as illustrated in (Figure 4c). Various types
28 of phase separation methods are available, including thermal-induced, solid-liquid and liquid-
29 liquid phase separation (60, 61).

30 The study by Kim et al. employed thermally induced phase separation (TIPS) for the
31 manufacture of poly(ethylene-glycol) (PEG) poly(L-lactic) acid (PLLA) scaffold to support
32 MC3T3-E1 osteoblast-like cells (62). It was shown in this study that ageing times and
33 temperature have a significant effect on the pores morphology of the fabricated scaffold,
34

1 quenching temperatures of 25°C, 30°C, and 35°C (Figure 8a-c). The TIPS technique allowed a
2 simple control of the scaffold pore size between 100 – 300 µm. Authors noted that MC3T3-E1
3 cells could proliferate successfully within 4 weeks after being seeded on the microporous
4 scaffold of PEG-PLLA (62).

5
6
7 The main merit of using the phase separation technique is that it does not require extra leaching.
8 However, the use of organic solutions like ethanol or methanol during the scaffold
9 manufacturing process can prevent the integration of bioactive compounds or cells.
10 Furthermore, the small pore diameters generated are another constraint for phase-separation
11 scaffolds. (43, 59).

12 13 **3.4. Freeze-drying**

14
15 Freeze-drying technique is based on a frozen liquid that sublime directly into the gas phase
16 leaving behind a porous hydrogel (Figure 4d) (63). The manufacturing approach was first
17 explored by Whang et al. to produce PLGA scaffolds (64). The literature demonstrates that
18 fabricated scaffolds' porosity and pore diameter are highly influenced by variables like the
19 water-to-polymer mixture ratio and the viscosity of the emulsion (59). Also, altering the cooling
20 temperature can control the scaffold's internal pore structure (65).

21 In a study conducted by Park et al. (66), freeze-drying was used to fabricate collagen and
22 hyaluronic acid (HA) membranes and then crosslinked using 1-ethyl-3-(3-
23 dimethylaminopropyl) carbodiimide (EDC). Porosity and pores' size were measured to assess
24 the effect of freezing temperature and crosslinking on the internal structure of the scaffolds,
25 freeze dried temperature used were at -20 ° C, -70 ° C, and -196 ° C (Figure 9a-c), (Table 2).
26 The higher the freezing temperatures, the larger the pore size and the porosity percentage. Also,
27 the use of EDC has significantly increased both the porosity and pore size. The prepared
28 membranes were safe and did not exhibit significant toxicity to L929 fibroblast cells upon
29 testing (66).

30
31 The main benefit of the freeze-drying technique is that it eliminates many rinsing processes by
32 immediately removing scattered water and polymer solutions (64). In addition, polymer liquids
33 can be utilised directly instead of any monomer crosslinking. Nevertheless, in order to increase

1 scaffold homogeneity, the freeze-drying method must be managed to minimise heterogeneous
2 freezing (65). Moreover, this approach is associated with high energy consumption, long
3 timescales, small irregular pores, and cytotoxic solvents (67, 68).

4 **3.5. Electrospinning**

5
6 Electrospinning is an innovative electrochemical technology that utilises an electrical charge to
7 create solid, nano-sized fibres from a liquid solution (69). As illustrated in (Figure 4e), the
8 electrospinning process begins with a syringe filled with a solution containing a precursor for
9 the nanofiber material and a connecting polymer being loaded onto a regulated syringe pump.
10 A metallic needle is attached to the syringe and is connected to a high-voltage power source
11 (70). As the solution flows through the metallic tip, it becomes electrified, generating a
12 deformed conical shape known as a Taylor cone. The Taylor cone's tip releases an electrified
13 fibre jet. As the solution travels to a grounded collector, the solvent evaporates, and the fibres
14 harden (70).

15 Wutticharoenmongkol et al. used electrospinning to create a 12% w/v PCL fibrous scaffold
16 with HA nanoparticle concentrations ranging between 0.5 and 1.0%. The porosity of the
17 constructed fibre scaffold increased by 82 and 90 %, and had pore sizes ranging from 4.3 to 5.6
18 μm . The prepared fibrous scaffolds had a tensile strength between 3.6 and 3.8 MPa (71).
19 Another study by He et al. reported the fabrication of a PCL/HA scaffold with different ratios
20 of PCL/0.3 HA, PCL/0.4 HA, and PCL/0.5 HA (Figure 10a-c) and an average pore size of 167
21 μm which is suitable for osteoblasts, by stacking meshes using near-field electrospinning (72).

22
23 Electrospinning has the advantage of being able to manipulate both the mechanical properties
24 and the porous structure of the fibre by regulating the voltages and distance between the syringe
25 and the collectors (73, 74). Pores generated by this approach, however, are often fewer than a
26 few tens of micrometres in size, making them unsuitable for tissue growth and cell culturing
27 (72). Also, fabricating complex geometry can be challenging using this technique.

28 **3.6. Self-assembly**

29
30 Self-assembly is the process by which the components of a system, whether molecules,
31 polymers, colloids, or macroscopic particles, arrange into ordered and/or functional structures
32 or patterns without external direction as a result of specific, local interactions among the
33 components (75). Collagen should be examined to better understand the origins and

1 significance of these structural features, as it is one of the most common proteins in the human
2 body. Collagen is formed within the cell as a triple helix structure by the assembly of three
3 distinct alpha strands (procollagen) (Figure 4f) (76). Procollagen is enzymatically broken to
4 generate tropocollagen, which combines and crosslinks with other tropocollagen molecules to
5 create the characteristic 67 nm banded fibrils after vesicle transit to the exterior of the cell (76).
6 This fibrillar structure is retained in collagen types I (skin, tendon, and bone), II (cartilage), and
7 III (skin, muscle) (76).

8 A recent study conducted by [88] demonstrated the self-assembly of a 3D porous Reduced
9 graphene oxide (RGO) composite scaffold that is composed of graphene oxide (GO) and nano-
10 hydroxyapatite (nHA) with pore sizes ranging from 20–100 μm (Figure 11) (77). The scaffold
11 significantly improved the proliferation, alkaline phosphatase activity (ALP), and osteogenic
12 gene expression of rat bone mesenchymal stem cells (rBMSCs) (77). Another study used a
13 combination of self-assembly and electrospinning techniques to create a hybrid scaffold with a
14 honeycomb using Polyhydroxybutyrate/poly(-caprolactone)/58S sol-gel bioactive glass
15 (PHB/PCL/58S) (78). The scaffold was created by changing the solution composition and
16 concentration during a single electrospinning process (78). The nanofiber contained pores as
17 small as a few micrometres in diameter, while the structure had pores ranging from 200 μm to
18 1000 μm . This facilitated the cell ingrowth and infiltration of MG-63 osteoblast-like cells into
19 the honeycomb-like scaffold (78).

20
21 The self-assembly mechanisms are frequently triggered by the mixing of two elements or by an
22 external stimulus (pH, ionic strength, or temperature), allowing these materials to be injected
23 or even used directly to encapsulate cells, compared to the complex processing needed for other
24 conventional manufacturing methods to fabricate a scaffold (76). In comparison to other
25 manufacturing processes, the mechanisms governing the development of self-assembled
26 nanofibers are generally more complex, requiring more careful molecular design and more
27 intricate synthesis. (Table 3) summarises the main applications, advantages and drawbacks of
28 the manufacturing techniques presented in this section.

29
30 From the literature review presented above, it can be concluded that conventional
31 manufacturing methods such as gas formation, salt leaching, freeze-drying, and phase
32 separation do not allow for accurate regulation of the internal scaffolding design or the
33 manufacture of complicated structures, which can be accomplished through AM modelled with

1 computer-aided design (CAD) (79). Besides, these conventional methods require good
2 manufacturing skills to maintain a consistent architecture of scaffolds. In addition, special care
3 must be taken to use toxic solvents that can lead to the death of cells if they are not removed
4 completely (80). Another limitation is that scaffolds manufactured in accordance with these
5 conventional processing methods have poor mechanical properties (81). Therefore, alternative
6 techniques such as 3D printing offer a good opportunity to avoid these issues.

7 **4. Three Dimensional Printers**

8
9 Industry 4.0, commonly known as digital technology, is revolutionising industries by making
10 factories smarter and assisting manufacturers in increasing quality, productivity, and
11 profitability. 3D printing is a manufacturing tool that has advanced over the last three decades
12 and is an essential component of digital technology. Charles Hull invented the technology in
13 1986, employing UV-sensitive polymers and ultraviolet light (UV) to generate three-
14 dimensional structures (82). Stereolithography Apparatus (SLA) was the name given to the
15 technology later on. Scientists and engineers have since developed a variety of unique 3D
16 printing techniques. The main advantage of these new technologies is that they enable the
17 fabrication of complex organic shapes and internal features and cavities in components that
18 were difficult or even impossible to fabricate with conventional techniques (83). Additional
19 benefits of 3D printing can include; reduced lead time, elimination of extra processing required
20 for mass customisation, develop supply chain expertise, printing systems and assemblies,
21 fabricating complicated designs in functional components, lightweight production of cellular
22 structures, material recycling and environmentally friendly production, scalable workflow, on-
23 demand production and enhanced service quality (83, 84). (Figure 12) summarises the most
24 employed 3D printing techniques. Binder Jetting, Fused Deposition Modelling, Selective Laser
25 Sintering and Stereolithography are the most employed for the manufacturing of scaffolds and,
26 therefore, will be discussed in detail in the following sections.

27 In regards to the bio-medical applications, the most significant benefit of 3D printing
28 technologies is allowing the fabrication of completely customised components. In 3D printing,
29 different materials such as polymers, metals, or ceramics can be created layer by layer to
30 produce the desired shape according to a computerised model, in contrast to typical
31 manufacturing or foaming procedures that demand removing and/or adding, such as cutting,
32 bending, and drilling (85). 3D printing technologies have been used in many industries, such as
33 biomedical, automotive, aerospace, defence, and many others. This is due to the capacity of
34 AM technologies to rapidly build complicated structures with precision and accuracy, as well

1 as the ability to recycle materials. Numerous researchers and industrial organisations have
2 focused their efforts on enabling the widespread implementation of 3D printing and
3 investigating its potential and limitations. (86-89). Therefore, 3D printing can play a major role
4 in the future of tissue engineering in general and bone scaffolds in particular. This is evident as
5 the number of studies employing 3D printing technology for bone scaffolds has increased over
6 the last decade (Figure 13).

7 **4.1. Binder jetting**

8
9 Binder jetting starts with a powder bed, the composition of which varies according to the
10 materials employed, which is dispersed over the building platform and flattened with the aid of
11 a roller system (90). Following that, the printer nozzle spreads binder solution in the powdery
12 regions indicated by the CAD. The excess powder is extracted (blown off) after the binder
13 solvent and powder are mixed. The building platform is then lowered, allowing for the deposit
14 and levelling of a new powder sheet (91). Following that, the process will be repeated till the
15 required design is fully fabricated (Figure 12a). After the layer deposition, the part generated
16 that is known as the green part usually has high porosity. In order to reduce the number of pores
17 and to improve its integrity, the component is subjected to cleaning and post-processing
18 operations: depowdering, debinding and finally, a sintering process in a furnace with densifying
19 and strengthening purposes.

20 In a study conducted by Zeltinger et al., chitosan and hydroxyapatite biocomposite scaffolds
21 were printed using a Z-Corp, Z-510 3D printer to create dense (solid, nonporous, 37.1%
22 porosity) and cylindrical scaffolds (92). These scaffolds were fabricated by applying a 40 wt%
23 lactic acid binder solution to various chitosan/hydroxyapatite composites (20 wt%, 25 wt%, and
24 30 wt% chitosan) followed by a post-hardening process. The authors observed that the scaffolds
25 printed with 25% chitosan had good mechanical properties, as evidenced by their compression
26 strength of 16.32 MPa and 4.4 GPa Young's modulus (92). Nevertheless, only the fabrication
27 of nonporous scaffolds has achieved the desired mechanical strength. In another study,
28 CALPHAD (Ca) and biodegradable Fe-Mn alloy were used to achieve higher decomposition
29 rates (Figure 14a-b) (93). The achieved ultimate tensile strength was 228.1 MPa for the Fe-Mn
30 and 296.6 MPa for the Fe-Mn-1Ca (93). During tensile testing, a brittle fracture occurred in a
31 porous Fe-Mn-1Ca scaffold with 52.9 % open porosity. Fe-Mn scaffolds with an open porosity
32 of 39.3 % had higher ductility than Fe-Mn-1Ca, demonstrating that scaffold Fe-based alloys
33 with less porosity have higher ductility (Figure 14c-d) (93). This is a concern since porosity is
34 a crucial feature as it promotes the diffusion of oxygen, nutrients, and cellular waste. The

1 availability and diversity of the powder-binder solutions make the binder jetting attractive for
2 manufacturing bone scaffold (90). On the other hand, a drawback of this technique is that it
3 needs post-processing, which may include heat treatment to assure durability (94).

4 **4.2. Materials jetting**

5
6 Materials jetting Printing (Bioplotter) is one of the most used 3D printing technologies for
7 cellular research due to the low temperature it requires and the low volume it uses (between 3
8 and 5 mL) (95). This technology is designed for high-precision printing of small objects using
9 small nozzles with a minimum diameter of 250 μm and low volume (96). The process starts by
10 loading the printing material in a semi-liquid or liquid form into the syringe. Then, pneumatic
11 pressure is applied to extrude the material through the printing nozzle (Figure 12b). The
12 materials are deposited in a layer-by-layer manner, and the process enables the combination of
13 different materials in each layer.

14 In the study by Poldervaart et al. VEGF was incorporated into a 3D printed matrigel-alginate
15 scaffold to promote vascularisation using BioScaffolder pneumatic dispensing system (97). The
16 incorporation of gelatin microparticles (GMPs) to sustainably regulate the release of VEGF led
17 to higher vascularisation compared to scaffolds with no growth factors and rapidly released
18 VEGF scaffolds when implemented in murine models (Figure 15). In another recent study, a
19 biphasic scaffold model was fabricated with the BioScaffolder by combining the unmodified
20 calcium phosphate cement (CPC) paste with a highly concentrated alginate-based hydrogel
21 paste that was embedded with VEGF by two-channel plotting within a single scaffold (98). The
22 scaffold was designed and manufactured to be used for evaluating a femur defect of size in the
23 range of 200 μm with a macro porosity of 57%. The scaffolds' size and high porosity made
24 them suitable for enhancing bone regeneration (98).

25 A unique feature of materials jetting processes is that it allows the printing of cell-laden gels to
26 deliver viable and usable scaffolds, often including other polymeric materials like PCL (99,
27 100). Another advantage of materials jetting is that it enables the growth factors such as platelet-
28 derived growth factor (PDGF) or vascular endothelial growth factor (VEGF) to be added to the
29 bio-ink to improve cell proliferation and differentiation which promotes angiogenesis (101).
30 Adding these growth factors will increase the tissue formation rate in scaffolds and generate
31 robust tissue as a result of increased differentiation. On the other hand, the shear stress from the
32 nozzles of various sizes can negatively impact cell viability (102).

4.3. Materials extrusion

In materials extrusion, thermoresponsive polymers are heated above their glass transition temperature and then placed on a solid surface. It uses a winding thermoplastic polymer filament that is unwound and extruded through a heated nozzle on a fabrication platform. The polymer solidifies and sets after contact with the platform (103). Upon depositing a layer, the process is repeated in a layer-by-layer process until the part is fully fabricated see (Figure 12c) (104).

Hong et al. employed a multi-head deposition method to combine PCL and PLGA to fabricate a multi-material scaffold with high compressive strength of 3.2 MPa and pore size of around 300 μm with 66.7% porosity (Figure 16). In combination with mussel adhesive proteins as a functional material, the fabricated scaffolds facilitated high cell attachment and proliferation of stem cells derived from human adipose tissue (105). It also yielded positive outcomes in vivo tests, where increased bone regeneration was observed in a calvarial defect of a rat model (105). Overall, FDM was mainly used in combination with other techniques or in indirect 3D printing for tissue engineering purposes.

The key disadvantages of FDM are that it enables multi-material and multi-colour fabrication processes within one component, and the accuracy can go down to ± 0.5 mm (106). However, it prevents any possible toxicity caused mainly by organic solvents that are required for the solubilisation of certain polymers, like dichloromethane, used to solubilise PLGA. The thermoplastic criterion for this technique restricts its application and adaptability in the production of scaffolds, as acrylonitrile butadiene styrene (ABS) is the most often utilised material. Other polymers have been used in FDM, like polycarbonate (PC), polyphenylsulfone (PPSF), and polyetherimide (PEI). However, these materials are not mainly used in tissue engineering applications. (107). Further investigation is needed to determine whether alternative thermoplastics, like polyesters, are suitable scaffolding materials for tissue engineering. Despite this drawback, FDM has been demonstrated to be a viable approach for manufacturing scaffolds for tissue engineering. Polyester, PLA, PCL, as well as PCL and PLA composites like PCL-TCP, HA - PCL and HA - PLA are the main option for FDM printed scaffolds (108-111).

4.4. Powder bed fusion

The laser powder bed fusion (L-PBF) technology begins with the powder layer being smeared on the surface of the base plate, followed by melting powdered particles together using a laser beam (normally a CO₂ laser) in the desired pattern (112). The process is repeated after the first layer is deposited, and then another layer is added on top of the pre-existing one (Figure 12d) (113, 114). The L-PBF technique was used to make scaffolds from biocompatible and biodegradable polymers like poly(lactic acid), polyvinyl alcohol, polycaprolactone, and polyetheretherketone (115). With the development of metal 3D printing, this technology is also employed for the fabrication of metallic scaffolds that can be created out of biocompatible metal alloys such as Ti6Al4V for the fabrication of implants (116).

The use of L-PBF for the manufacturing of scaffolds has been studied by many researchers in the literature. Liu et al. utilised hydroxyapatite (HA), sodium tripolyphosphate and silica sol biocomposite slurry to manufacture scaffolds using L-PBF with different heat treatment temperatures at ambient temperature, 1200 °C, 1300 °C, and 1400 °C (Figure 17a-d). These scaffolds showed significant mechanical strength (up to 43.26 MPa) but had low porosity with a pores size of 5-25 µm. The in vitro research, however, suggested the possibility of using these scaffolds for osteoblast growth, such as cells (117). In another study by I. Gibson, the authors optimised the laser beam power, scan spacing and laser thickness to fabricate a nanocomposite scaffold made of poly(hydroxybutyrate-co-hydroxyvalerate) and calcium phosphate (118). The analysed parameters were found to have a substantial effect on the mechanical properties of the scaffold; compressive properties, precision, and durability (119). Nevertheless, the scaffold's efficiency and utility must be evaluated in vitro and in vivo. Other scholars have fabricated a scaffold using bioresorbable polycaprolactone (PCL) at high precision and high compression moduli ranging from 52-67 MPa. The scaffold was loaded with bone morphogenetic protein-7 (BMP7), and has demonstrated bone generation in vivo (120).

When low porosity and high mechanical strength are needed, the use of L-PBF processes can be beneficial; nonetheless, the need for powdered material to be able to withstand laser heat and resistant shrinking throughout the melting process are some limitations of this technique. Another drawback of L-PBF is the pre-heating and post-heating treatments of the powdered material among the crystallisation glass transition or melting temperatures to lower the shrinking of the scaffolds induced by the laser (117, 121).

4.5. Vat photopolymerization

Vat photopolymerisation or stereolithography (SLA) technique is based on the fabrication of components from a liquid polymer via a chemical reaction mediated by light. A photocurable polymer is placed on a surface medium and then subjected to UV radiation in the 300–400 nm wavelength range, forming the first layer (Figure 12e) (122). After the initial layer has been hardened, the process is repeated, overlaying the preceding layer until the part is completely fabricated (123, 124). SLA biomaterials include polypropylene fumarate (PPF) with photocross linkers and polyethylene glycol acrylate.

A study conducted by Cooke et al. used the (SLA 250/40) stereolithography for Printing (PPF) scaffolds together with Irgacure 819 photoinitiator. The manufactured scaffolds had a porosity of 90% and a pore size range of 150–800 μm (125, 126). Their study demonstrated the possibility of fabricating scaffolds using (PPF) material (Figure 18). However, in vitro and vivo studies must be carried out to determine the scaffold cytotoxicity and biocompatibility. Despite the magnificent results that SLA can achieve in terms of complex geometries fabrication, Various novel biodegradable and biocompatible photocurable polymers must be developed. In addition, designing and improving visible light-based STA systems is important in order to have a list of polymeric materials (125).

The advantage of the SLA technology is that it allows for precise control and fabrication of high-resolution detailed scaffold geometries that almost perfectly mimic the CAD model. Nonetheless, due to the use of an extra curing phase to enhance the properties of the prototype, the final resolution is affected by the shrinkage usually occurring in the post-processing phase (127, 128). However, the drawback of SLA techniques is that it uses only photopolymers that use photoinitiators (129). In addition, the majority of photoinitiators include radical photopolymerisation by photocleavage, hydrogen extraction, and cationic photopolymerisation, with cationic photoinitiators being incompatible with biomedical applications because of the formation of toxic byproducts. Also, the widely used ultraviolet light source for the polymerisation process poses another risk as reports indicate that this light source is harmful to our DNA cells and might be a potential cause of skin cancer (130, 131). (Table 4) summarises the various 3D printing techniques used in preparing bone scaffolds.

4.6 Directed energy deposition and Sheet lamination

The directed energy deposition (DED) technology fabricates the required object by melting materials using a laser beam while using a nozzle to deposit the material in specific locations, as demonstrated in (Figure 12f) (132). It mostly uses metal types of materials, such as stainless steel, aluminum, or copper, in the form of powder or wire (133). This technique usually require post-processing due to distortions in the fabricated part (134). Due to the limited types of materials that can be processed and the poor quality of the fabrication, this technique has not been utilized much in biomedical applications

In sheet lamination (SL), a sheet material is laminated in a layer-by-layer manner and cut using a laser beam to fabricate the required object as demonstrated in (Figure 12g). It uses different types of materials such as paper, metal, and plastic (135). Similarly to directed energy deposition, sheet lamination has not been widely used in biomedical applications due to its poor fabrication quality, the need for post-processing, and the difficulty in fabricating complex shapes using this technique (136).

1 In general, both manufacturing technologies have different advantages and disadvantages,
2 primarily depending on the application of the fabricated object. For example, when complex
3 geometries and designs are required, additive manufacturing technology has proven to be a
4 better option than conventional manufacturing as it allows for the creation of internal structures
5 (137). In contrast, conventional manufacturing is more precise, can handle a wider variety of
6 materials, and is better suited for large-scale production than additive manufacturing (138).
7 Additive manufacturing is a relatively new technology that is still being developed and has
8 limitations regarding the types of materials it can process and the size of the components it can
9 produce (138). In fact, researchers have combined conventional and additive manufacturing
10 technologies into a single machine for bone scaffold fabrication, effectively combining their
11 respective advantages.

12 The research conducted by Jiankang He and his team, a new printing method was developed
13 that combines FDM and electrospinning technologies to create 3D tissue-engineered scaffolds
14 with intricate curved shapes and microscale fibrous structures (Figure 19a). The melting
15 temperature was optimized to print PCL filaments of around 10 μm , which were stacked to
16 create 3D walls with smooth surface (139). By adjusting the stage movement speed and
17 direction, they were able to print PCL scaffolds with curved outlines, predefined fiber spacing,
18 and orientations at 90° and 45° (Figure 19b-g). Biological experiments demonstrated that the
19 printed microscale scaffolds were biocompatible and promoted in vitro cellular proliferation
20 and alignment (139). In another research conducted by H. Hassanin et al., they successfully
21 produced micro implantable components with the highest density and best surface quality
22 possible by utilizing a hybrid microfabrication technology that incorporates the design
23 flexibility of SLM and the exceptional surface quality of $\mu\text{-EDM}$ (140). Another group of
24 researchers has developed a new approach to create three-dimensional graphene (3DG)
25 composites scaffold by combining selective laser melting (SLM) and chemical vapor deposition
26 (CVD) techniques (141). They fabricated a 3D porous copper template using SLM and grew
27 graphene in-situ via CVD on the template. This technique allowed for accurate control of the
28 design and regulation of 3DG, resulting in enhanced electromagnetic interference (EMI)
29 shielding and improved thermal diffusion (141).

30 31 **5. Conclusions**

32
33 This paper presents a literature review of the most relevant works and recent advances
34 concerning manufacturing bone scaffolds. Conventional manufacturing techniques have been

1 reviewed, and their main benefits and shortcomings have been addressed. Additionally, 3D
2 printing technologies that have emerged in the last years have proved to be a feasible alternative.
3 In this context, the review demonstrated that 3D printing technologies enable the customisation
4 of bone scaffolds to meet individual patients' unique needs and health situations. Progress in
5 this area is facilitated by advancements in computer-aided design (CAD) and computer-aided
6 manufacturing (CAM), which enable rapid and precise organ scanning and design. The
7 scaffold's structural properties, such as pore size and porosity, have a direct influence on their
8 functionality in both vitro and vivo. In general, interconnected porous scaffolding networks that
9 allow nutrient transport and waste disposal and promote cell migration and proliferation are
10 significant. Pore size and porosity affect the behaviour of the cells and determine the overall
11 mechanical properties of the scaffold. Presently, the concept of fabricating scaffolds is
12 concentrated on generating materials with suitable pore size, structure, and porosity for specific
13 uses. Typically, scaffolds are 3D printed, and cells are grown in/on these scaffolds. One of the
14 challenges of 3D printing is using non-biocompatible materials in several 3D printing
15 techniques, such as binders or photoinhibitors, even after the high-temperature debinding or
16 sintering process. These components cannot remove entirely after heating or sintering processes
17 and may compromise the biocompatibility of the constructs. Also, applying the temperature in
18 some of the technologies restricts the applicability of materials. Incompatibility of the cellular
19 application with the scaffold would gradually cause the entire scaffolding system to fail.

20 In addition, 3D printing technology has altered the way bone fractures and has enabled the
21 utilisation of drug-loaded implants and/or scaffolds of complicated geometries and high
22 resolution to accelerate the healing procedure and recover bone structure and toughness. Bone
23 scaffolds have been extensively manufactured using techniques like FDM and binder jetting.
24 FDM has been demonstrated to be capable of processing a wide variety of scaffolds with
25 complicated structures and a variety of polymeric materials. On the other hand, techniques like
26 directed energy deposition and sheet lamination (Figure 12f-g) were not explored in this field
27 due to their processing characteristics or the quality of their products or materials. Clinical trials
28 conducted by academia or commerce on the developed systems demonstrate significant
29 potential. However, challenges such as materials recycling, quality control, and the effect of
30 inherited issues of 3D printing such as surface roughness, internal defects, and post-processing
31 are still lacking.

1 References

1. Wu A-M, Bisignano C, James SL, et al. Global, regional, and national burden of bone fractures in 204 countries and territories, 1990–2019: a systematic analysis from the Global Burden of Disease Study 2019. *Lancet Healthy Longev.* 2021;2(9):e580-e92.
2. Hassanin H, Al-Kinani AA, ElShaer A, et al. Stainless steel with tailored porosity using canister-free hot isostatic pressing for improved osseointegration implants. *Journal of Materials Chemistry B.* 2017;5(47):9384-94.
3. Heuijers A, Wilson W, Ito K, et al. The critical size of focal articular cartilage defects is associated with strains in the collagen fibers. *Clin Biomech (Bristol, Avon).* 2017;50:40-6.
4. Yang Y, Wu P, Wang Q, et al. The Enhancement of Mg Corrosion Resistance by Alloying Mn and Laser-Melting. *Materials (Basel).* 2016;9(4).
5. Wang Z, Wang C, Li C, et al. Analysis of factors influencing bone ingrowth into three-dimensional printed porous metal scaffolds: a review. *Journal of Alloys and Compounds.* 2017;717:271-85.
6. Kumar A, Mandal S, Barui S, et al. Low temperature additive manufacturing of three dimensional scaffolds for bone-tissue engineering applications: Processing related challenges and property assessment. *Mater Sci Eng R Rep.* 2016;103:1-39.
7. Janik H, Marzec M. A review: fabrication of porous polyurethane scaffolds. *Mater Sci Eng C Mater Biol Appl.* 2015;48:586-91.
8. Bose S, Ke D, Sahasrabudhe H, et al. Additive manufacturing of biomaterials. *Progress in materials science.* 2018;93:45-111.
9. Gao C, Peng S, Feng P, et al. Bone biomaterials and interactions with stem cells. *Bone Res.* 2017;5(1):17059.
10. Currey JD. The structure and mechanics of bone. *J Mater Sci.* 2012;47(1):41-54.
11. Lacroix D. 4 - Biomechanical aspects of bone repair. In: Planell JA, Best SM, Lacroix D, Merolli A, editors. *Bone Repair Biomaterials: Woodhead Publishing; 2009.* p. 106-18.
12. Hasegawa K, Turner CH, Burr DB. Contribution of collagen and mineral to the elastic anisotropy of bone. *Calcified Tissue International.* 1994;55(5):381-6.
13. Frost HM. Some ABC's of skeletal pathophysiology. 6. The growth/modeling/remodeling distinction. *Calcified Tissue International.* 1991;49(5):301-2.
14. Parfitt AM. Chapter 15 - Skeletal Heterogeneity and the Purposes of Bone Remodeling: Implications for the Understanding of Osteoporosis. In: Marcus R, Feldman D, Kelsey J, editors. *Osteoporosis (Second Edition).* San Diego: Academic Press; 2001. p. 433-47.
15. Lacroix D. 3 - Biomechanical aspects of bone repair. In: Pawelec KM, Planell JA, editors. *Bone Repair Biomaterials (Second Edition): Woodhead Publishing; 2019.* p. 53-64.
16. Mach DB, Rogers SD, Sabino MC, et al. Origins of skeletal pain: sensory and sympathetic innervation of the mouse femur. *Neuroscience.* 2002;113(1):155-66.
17. Bjørnerem Å. The clinical contribution of cortical porosity to fragility fractures. *Bonekey Rep.* 2016;5:846-.
18. Schaffler MB, Radin EL, Burr DB. Mechanical and morphological effects of strain rate on fatigue of compact bone. *Bone.* 1989;10(3):207-14.

19. Fuchs RK, Thompson WR, Warden SJ. 2 - Bone biology. In: Pawelec KM, Planell JA, editors. *Bone Repair Biomaterials (Second Edition)*: Woodhead Publishing; 2019. p. 15-52.
20. Mow VC, Ratcliffe A, Woo SLY. *Biomechanics of Diarthrodial Joints*: Springer New York; 2012.
21. Gibson LJ. The mechanical behaviour of cancellous bone. *Journal of Biomechanics*. 1985;18(5):317-28.
22. Ding M, Dalstra M, Danielsen C, et al. Age variations in the properties of human tibial trabecular bone. *J Bone Joint Surg Br*. 1997;79:995-1002.
23. Melvin JW. *Fracture Mechanics of Bone*. *Journal of Biomechanical Engineering*. 1993;115(4B):549-54.
24. Kumar P, Vinitha B, Fathima G. Bone grafts in dentistry. *J Pharm Bioallied Sci*. 2013;5(Suppl 1):S125-S7.
25. Brydone AS, Meek D, Maclaine S. Bone grafting, orthopaedic biomaterials, and the clinical need for bone engineering. *Proc Inst Mech Eng H*. 2010;224(12):1329-43.
26. Dimitriou R, Jones E, McGonagle D, et al. Bone regeneration: current concepts and future directions. *BMC Medicine*. 2011;9(1):66.
27. Moshiri A, Oryan A. Role of tissue engineering in tendon reconstructive surgery and regenerative medicine: current concepts, approaches and concerns. *Hard Tissue*. 2012;1(2):11.
28. Oryan A, Moshiri A. Recombinant fibroblast growth protein enhances healing ability of experimentally induced tendon injury in vivo. *Journal of Tissue Engineering and Regenerative Medicine*. 2014;8(6):421-31.
29. Oryan A, Moshiri A. A long term study on the role of exogenous human recombinant basic fibroblast growth factor on the superficial digital flexor tendon healing in rabbits. *J Musculoskelet Neuronal Interact*. 2011;11(2):185-95.
30. Parizi AM, Oryan A, Shafiei-Sarvestani Z, et al. Human platelet rich plasma plus Persian Gulf coral effects on experimental bone healing in rabbit model: radiological, histological, macroscopical and biomechanical evaluation. *Journal of Materials Science: Materials in Medicine*. 2012;23(2):473-83.
31. Oryan A, Meimandi Parizi A, Shafiei-Sarvestani Z, et al. Effects of combined hydroxyapatite and human platelet rich plasma on bone healing in rabbit model: radiological, macroscopical, histopathological and biomechanical evaluation. *Cell Tissue Bank*. 2012;13(4):639-51.
32. Shafiei-Sarvestani Z, Oryan A, Bigham AS, et al. The effect of hydroxyapatite-hPRP, and coral-hPRP on bone healing in rabbits: Radiological, biomechanical, macroscopic and histopathologic evaluation. *Int J Surg*. 2012;10(2):96-101.
33. Oryan A, Moshiri A, Raayat AR. Novel Application of Theranekron® Enhanced the Structural and Functional Performance of the Tenotomized Tendon in Rabbits. *Cells Tissues Organs*. 2012;196(5):442-55.
34. Zimmermann G, Moghaddam A. Allograft bone matrix versus synthetic bone graft substitutes. *Injury*. 2011;42:S16-S21.
35. Janicki P, Schmidmaier G. What should be the characteristics of the ideal bone graft substitute? Combining scaffolds with growth factors and/or stem cells. *Injury*. 2011;42:S77-S81.
36. Oryan A, Moshiri A, Sharifi P. Advances in injured tendon engineering with emphasis on the role of collagen implants. *Hard Tissue*. 2012;1(2):12.
37. Oryan A, Alidadi S, Moshiri A. Current concerns regarding healing of bone defects. *Hard tissue*. 2013;2(2):1-12.

- 1 38. Athanasiou VT, Papachristou DJ, Panagopoulos A, et al. Histological
2 comparison of autograft, allograft-DBM, xenograft, and synthetic grafts in a trabecular
3 bone defect: an experimental study in rabbits. *Medical Science Monitor*.
4 2009;16(1):BR24-BR31.
- 5 39. Putzier M, Strube P, Funk JF, et al. Allogenic versus autologous cancellous
6 bone in lumbar segmental spondylodesis: a randomized prospective study. *European*
7 *Spine Journal*. 2009;18(5):687-95.
- 8 40. Roberts TT, Rosenbaum AJ. Bone grafts, bone substitutes and orthobiologics:
9 the bridge between basic science and clinical advancements in fracture healing.
10 *Organogenesis*. 2012;8(4):114-24.
- 11 41. Bajaj P, Schweller RM, Khademhosseini A, et al. 3D biofabrication strategies
12 for tissue engineering and regenerative medicine. *Annual review of biomedical*
13 *engineering*. 2014;16:247-76.
- 14 42. Thavornyutikarn B, Chantarapanich N, Sitthiseripratip K, et al. Bone tissue
15 engineering scaffolding: computer-aided scaffolding techniques. *Prog Biomater*.
16 2014;3(2-4):61-102.
- 17 43. Ma PX. Scaffolds for tissue fabrication. *Materials Today*. 2004;7(5):30-40.
- 18 44. Ma PX, Langer R. Fabrication of Biodegradable Polymer Foams for Cell
19 Transplantation and Tissue Engineering. In: Morgan JR, Yarmush ML, editors. *Tissue*
20 *Engineering Methods and Protocols*. Totowa, NJ: Humana Press; 1999. p. 47-56.
- 21 45. Lu L, Peter SJ, Lyman MD, et al. In vitro degradation of porous poly(L-lactic
22 acid) foams. *Biomaterials*. 2000;21(15):1595-605.
- 23 46. Lee SB, Kim YH, Chong MS, et al. Study of gelatin-containing artificial skin V:
24 fabrication of gelatin scaffolds using a salt-leaching method. *Biomaterials*.
25 2005;26(14):1961-8.
- 26 47. Lee SB, Kim YH, Chong MS, et al. Preparation and characteristics of hybrid
27 scaffolds composed of β -chitin and collagen. *Biomaterials*. 2004;25(12):2309-17.
- 28 48. Tessmar J, Holland T, Mikos A. Salt Leaching for Polymer Scaffolds. 2005. p.
29 111-24.
- 30 49. Thavornyutikarn B, Chantarapanich N, Sitthiseripratip K, et al. Bone tissue
31 engineering scaffolding: computer-aided scaffolding techniques. *Progress in*
32 *Biomaterials*. 2014;3(2):61-102.
- 33 50. Subia B, Kundu J, Kundu SC. Biomaterial scaffold fabrication techniques for
34 potential tissue engineering applications. *Tissue engineering*. 2010;141.
- 35 51. Quirk RA, France RM, Shakesheff KM, et al. Supercritical fluid technologies
36 and tissue engineering scaffolds. *Current Opinion in Solid State and Materials*
37 *Science*. 2004;8(3):313-21.
- 38 52. Zellander A, Gemeinhart R, Djalilian A, et al. Designing a gas foamed scaffold
39 for keratoprosthesis. *Mater Sci Eng C Mater Biol Appl*. 2013;33(6):3396-403.
- 40 53. Haugen H, Ried V, Brunner M, et al. Water as foaming agent for open cell
41 polyurethane structures. *Journal of Materials Science: Materials in Medicine*.
42 2004;15(4):343-6.
- 43 54. Mooney DJ, Baldwin DF, Suh NP, et al. Novel approach to fabricate porous
44 sponges of poly(d,l-lactic-co-glycolic acid) without the use of organic solvents.
45 *Biomaterials*. 1996;17(14):1417-22.
- 46 55. Kim HJ, Park IK, Kim JH, et al. Gas foaming fabrication of porous biphasic
47 calcium phosphate for bone regeneration. *Tissue Eng Regen Med*. 2012;9(2):63-8.
- 48 56. Nam YS, Yoon JJ, Park TG. A novel fabrication method of macroporous
49 biodegradable polymer scaffolds using gas foaming salt as a porogen additive. *J*
50 *Biomed Mater Res*. 2000;53(1):1-7.

- 1 57. Keskar V, Marion NW, Mao JJ, et al. In Vitro Evaluation of Macroporous
2 Hydrogels to Facilitate Stem Cell Infiltration, Growth, and Mineralization. *Tissue Eng*
3 Part A. 2009;15(7):1695-707.
- 4 58. Wachiralarpphaithoon C, Iwasaki Y, Akiyoshi K. Enzyme-degradable
5 phosphorylcholine porous hydrogels cross-linked with polyphosphoesters for cell
6 matrices. *Biomaterials*. 2007;28(6):984-93.
- 7 59. Mikos AG, Temenoff JS. Formation of highly porous biodegradable scaffolds
8 for tissue engineering. *Electronic Journal of Biotechnology*. 2000;3:23-4.
- 9 60. Nam YS, Park TG. Porous biodegradable polymeric scaffolds prepared by
10 thermally induced phase separation. *J Biomed Mater Res*. 1999;47(1):8-17.
- 11 61. Schugens C, Maquet V, Grandfils C, et al. Polylactide macroporous
12 biodegradable implants for cell transplantation. II. Preparation of polylactide foams by
13 liquid-liquid phase separation. *J Biomed Mater Res*. 1996;30(4):449-61.
- 14 62. Kim HD, Bae EH, Kwon IC, et al. Effect of PEG-PLLA diblock copolymer on
15 macroporous PLLA scaffolds by thermally induced phase separation. *Biomaterials*.
16 2004;25(12):2319-29.
- 17 63. Czernuszka SE. JT Making tissue engineering scaffolds work. Review: the
18 application of solid freeform fabrication technology to the production of tissue
19 engineering scaffolds. *Eur Cell Mater*. 2003;5:29-39.
- 20 64. Whang K, Thomas CH, Healy KE, et al. A novel method to fabricate
21 bioabsorbable scaffolds. *Polymer*. 1995;36(4):837-42.
- 22 65. O'Brien FJ, Harley BA, Yannas IV, et al. Influence of freezing rate on pore
23 structure in freeze-dried collagen-GAG scaffolds. *Biomaterials*. 2004;25(6):1077-86.
- 24 66. Park S-N, Park J-C, Kim HO, et al. Characterization of porous
25 collagen/hyaluronic acid scaffold modified by 1-ethyl-3-(3-
26 dimethylaminopropyl)carbodiimide cross-linking. *Biomaterials*. 2002;23(4):1205-12.
- 27 67. Bajaj P, Schweller RM, Khademhosseini A, et al. 3D Biofabrication Strategies
28 for Tissue Engineering and Regenerative Medicine. *Annual Review of Biomedical*
29 *Engineering*. 2014;16(1):247-76.
- 30 68. Zhu N, Chen X. Biofabrication of tissue scaffolds. *Advances in biomaterials*
31 *science and biomedical applications*. 2013:315-28.
- 32 69. Ramakrishna S, Fujihara K, Teo W-E, et al. An Introduction to Electrospinning
33 and Nanofibers: WORLD SCIENTIFIC; 2005. 396 p.
- 34 70. Nalbandian M. Development and Optimization of Chemically-Active
35 Electrospun Nanofibers for Treatment of Impaired Water Sources 2014.
- 36 71. Wutticharoenmongkol P, Sanchavanakit N, Pavasant P, et al. Novel bone
37 scaffolds of electrospun polycaprolactone fibers filled with nanoparticles. *J Nanosci*
38 *Nanotechnol*. 2006;6(2):514-22.
- 39 72. He F-L, Li D-W, He J, et al. A novel layer-structured scaffold with large pore
40 sizes suitable for 3D cell culture prepared by near-field electrospinning. *Mater Sci*
41 *Eng C Mater Biol Appl*. 2018;86:18-27.
- 42 73. Dhand C, Ong ST, Dwivedi N, et al. Bio-inspired in situ crosslinking and
43 mineralization of electrospun collagen scaffolds for bone tissue engineering.
44 *Biomaterials*. 2016;104:323-38.
- 45 74. Thavasi V, Singh G, Ramakrishna S. Electrospun nanofibers in energy and
46 environmental applications. *Energy & Environmental Science*. 2008;1(2):205-21.
- 47 75. Varga M. Chapter 3 - Self-assembly of nanobiomaterials. In: Grumezescu AM,
48 editor. *Fabrication and Self-Assembly of Nanobiomaterials*: William Andrew
49 Publishing; 2016. p. 57-90.
- 50 76. Wade RJ, Burdick JA. Advances in nanofibrous scaffolds for biomedical
51 applications: From electrospinning to self-assembly. *Nano Today*. 2014;9(6):722-42.

- 1 77. Nie W, Peng C, Zhou X, et al. Three-dimensional porous scaffold by self-
2 assembly of reduced graphene oxide and nano-hydroxyapatite composites for bone
3 tissue engineering. *Carbon*. 2017;116:325-37.
- 4 78. Ding Y, Li W, Schubert DW, et al. An organic-inorganic hybrid scaffold with
5 honeycomb-like structures enabled by one-step self-assembly-driven electrospinning.
6 *Mater Sci Eng C Mater Biol Appl*. 2021;124:112079.
- 7 79. Liu Tsang V, Bhatia SN. Three-dimensional tissue fabrication. *Advanced Drug*
8 *Delivery Reviews*. 2004;56(11):1635-47.
- 9 80. Yeong W-Y, Chua C-K, Leong K-F, et al. Rapid prototyping in tissue
10 engineering: challenges and potential. *Trends in Biotechnology*. 2004;22(12):643-52.
- 11 81. Hollister SJ. Porous scaffold design for tissue engineering. *Nat Mater*.
12 2005;4(7):518-24.
- 13 82. Mohammed A, Elshaer A, Sareh P, et al. Additive Manufacturing Technologies
14 for Drug Delivery Applications. *International Journal of Pharmaceutics*.
15 2020;580:119245.
- 16 83. Pieterse FF, Nel AL, editors. The advantages of 3D printing in undergraduate
17 mechanical engineering research. 2016 IEEE Global Engineering Education
18 Conference (EDUCON); 2016 10-13 April 2016.
- 19 84. Berman B. 3-D printing: The new industrial revolution. *Business Horizons*.
20 2012;55(2):155-62.
- 21 85. Klippstein H, Diaz De Cerio Sanchez A, Hassanin H, et al. Fused Deposition
22 Modeling for Unmanned Aerial Vehicles (UAVs): A Review. *Advanced Engineering*
23 *Materials*. 2018;20(2):1700552.
- 24 86. Essa K, Hassanin H, Attallah MM, et al. Development and testing of an
25 additively manufactured monolithic catalyst bed for HTP thruster applications. *Appl*
26 *Catal A Gen*. 2017;542:125-35.
- 27 87. Qiu C, Adkins NJE, Hassanin H, et al. In-situ shelling via selective laser
28 melting: Modelling and microstructural characterisation. *Mater Des*. 2015;87:845-53.
- 29 88. Sabouri A, Yetisen AK, Sadigzade R, et al. Three-Dimensional Microstructured
30 Lattices for Oil Sensing. *Energy & Fuels*. 2017;31(3):2524-9.
- 31 89. Klippstein H, Hassanin H, Diaz De Cerio Sanchez A, et al. Additive
32 Manufacturing of Porous Structures for Unmanned Aerial Vehicles Applications.
33 *Advanced Engineering Materials*. 2018;20(9):1800290.
- 34 90. Ferrari A, Frank D, Hennen L, et al. Additive bio-manufacturing: 3D printing for
35 medical recovery and human enhancement 2018.
- 36 91. Ziaee M, Crane NB. Binder jetting: A review of process, materials, and
37 methods. *Addit Manuf*. 2019;28:781-801.
- 38 92. Chavanne P, Stevanovic S, Wüthrich A, et al. 3D printed chitosan /
39 hydroxyapatite scaffolds for potential use in regenerative medicine. *Biomed Tech*
40 *(Berl)* 2013.
- 41 93. Hong D, Chou D-T, Velikokhatnyi OI, et al. Binder-jetting 3D printing and alloy
42 development of new biodegradable Fe-Mn-Ca/Mg alloys. *Acta Biomater*.
43 2016;45:375-86.
- 44 94. Mostafaei A, Elliott AM, Barnes JE, et al. Binder jet 3D printing—Process
45 parameters, materials, properties, modeling, and challenges. *Progress in Materials*
46 *Science*. 2021;119:100707.
- 47 95. Lim SH, Kathuria H, Tan JJY, et al. 3D printed drug delivery and testing
48 systems — a passing fad or the future? *Advanced Drug Delivery Reviews*.
49 2018;132:139-68.
- 50 96. Pusch K, Hinton TJ, Feinberg AW. Large volume syringe pump extruder for
51 desktop 3D printers. *HardwareX*. 2018;3:49-61.

- 1
2
3 1 97. Poldervaart MT, Gremmels H, van Deventer K, et al. Prolonged presence of
4 2 VEGF promotes vascularization in 3D bioprinted scaffolds with defined architecture. *J*
5 3 *Control Release*. 2014;184:58-66.
6 4
7 4 98. Ahlfeld T, Akkineni AR, Förster Y, et al. Design and Fabrication of Complex
8 5 Scaffolds for Bone Defect Healing: Combined 3D Plotting of a Calcium Phosphate
9 6 Cement and a Growth Factor-Loaded Hydrogel. *Annals of Biomedical Engineering*.
10 7 2017;45(1):224-36.
11 8
12 9 99. Whulanza Y, Arsyah R, Saragih A. Characterization of hydrogel printer for
13 10 direct cell-laden scaffolds 2018. 040002 p.
14 11
15 10 100. Negro A, Cherbuin T, Lutolf M. 3D Inkjet Printing of Complex, Cell-Laden
16 12 Hydrogel Structures. *Scientific Reports*. 2018;8.
17 13
18 12 101. Wei L, Wu S, Kuss M, et al. 3D printing of silk fibroin-based hybrid scaffold
19 14 treated with platelet rich plasma for bone tissue engineering. *Bioact Mater*.
20 15 2019;4:256-60.
21 16
22 15 102. Ozbolat IT, Chen H, Yu Y. Development of 'Multi-arm Bioprinter' for hybrid
23 17 biofabrication of tissue engineering constructs. *Robot Comput Integr Manuf*.
24 18 2014;30(3):295-304.
25 19
26 18 103. Ngo TD, Kashani A, Imbalzano G, et al. Additive manufacturing (3D printing):
27 19 A review of materials, methods, applications and challenges. *Compos B Eng*.
28 20 2018;143:172-96.
29 21
30 21 104. Langford T, Mohammed A, Essa K, et al. 4D Printing of Origami Structures for
31 22 Minimally Invasive Surgeries Using Functional Scaffold. *Applied Sciences [Internet]*.
32 23 2021; 11(1).
33 24
34 24 105. Hong JM, Kim BJ, Shim J-H, et al. Enhancement of bone regeneration through
35 25 facile surface functionalization of solid freeform fabrication-based three-dimensional
36 26 scaffolds using mussel adhesive proteins. *Acta Biomater*. 2012;8(7):2578-86.
37 27
38 27 106. Ferrari A, Frank D, Hennen L, et al. Additive bio-manufacturing: 3D printing for
39 28 medical recovery and human enhancement 2018.
40 29
41 29 107. Wong KV, Hernandez A. A review of additive manufacturing. *ISRN Mechanical*
42 30 *Engineering*. 2012;2012.
43 31
44 31 108. Zein I, Hutmacher DW, Tan KC, et al. Fused deposition modeling of novel
45 32 scaffold architectures for tissue engineering applications. *Biomaterials*.
46 33 2002;23(4):1169-85.
47 34
48 34 109. Water JJ, Bohr A, Boetker J, et al. Three-Dimensional Printing of Drug-Eluting
49 35 Implants: Preparation of an Antimicrobial Polylactide Feedstock Material. *Journal of*
50 36 *Pharmaceutical Sciences*. 2015;104(3):1099-107.
51 37
52 37 110. Sandler N, Salmela I, Fallarero A, et al. Towards fabrication of 3D printed
53 38 medical devices to prevent biofilm formation. *International Journal of Pharmaceutics*.
54 39 2014;459(1):62-4.
55 40
56 40 111. Melčová V, Svoradová K, Menčík P, et al. FDM 3D Printed Composites for
57 41 Bone Tissue Engineering Based on Plasticized Poly(3-hydroxybutyrate)/poly(d,l-
58 42 lactide) Blends. *Polymers (Basel)*. 2020;12(12).
59 43
60 43 112. Bittredge O, Hassanin H, El-Sayed MA, et al. Fabrication and Optimisation of
61 44 Ti-6Al-4V Lattice-Structured Total Shoulder Implants Using Laser Additive
62 45 Manufacturing. *Materials [Internet]*. 2022; 15(9).
63 46
64 46 113. Elsayed M, Ghazy M, Youssef Y, et al. Optimization of SLM process
65 47 parameters for Ti6Al4V medical implants. *Rapid Prototyping Journal*. 2019;25(3):433-
66 48 47.
67 49
68 49 114. El-Sayed MA, Essa K, Ghazy M, et al. Design optimization of additively
69 50 manufactured titanium lattice structures for biomedical implants. *The International*
70 51 *Journal of Advanced Manufacturing Technology*. 2020;110(9):2257-68.

- 1 115. Kusoglu I, Doñate-Buendía C, Barcikowski S, et al. Laser Powder Bed Fusion
2 of Polymers: Quantitative Research Direction Indices. *Materials (Basel, Switzerland)*.
3 2021;14.
- 4 116. Gaur B, Soman D, Ghyar R, et al. Ti6Al4V scaffolds fabricated by laser
5 powder bed fusion with hybrid volumetric energy density. *Rapid Prototyp J*. 2022.
- 6 117. Liu F-H. Synthesis of biomedical composite scaffolds by laser sintering:
7 Mechanical properties and in vitro bioactivity evaluation. *Applied Surface Science*.
8 2014;297:1-8.
- 9 118. Gibson I. Material properties and fabrication parameters in selective laser
10 sintering process. *Rapid Prototyp J*. 1997;3(4):129-36.
- 11 119. Duan B, Cheung WL, Wang M. Optimized fabrication of Ca–P/PHBV
12 nanocomposite scaffolds via selective laser sintering for bone tissue engineering.
13 *Biofabrication*. 2011;3(1):015001.
- 14 120. Williams JM, Adewunmi A, Schek RM, et al. Bone tissue engineering using
15 polycaprolactone scaffolds fabricated via selective laser sintering. *Biomaterials*.
16 2005;26(23):4817-27.
- 17 121. Kruth JP, Levy G, Klocke F, et al. Consolidation phenomena in laser and
18 powder-bed based layered manufacturing. *CIRP Ann Manuf Technol*.
19 2007;56(2):730-59.
- 20 122. Park HK, Shin M, Kim B, et al. A visible light-curable yet visible wavelength-
21 transparent resin for stereolithography 3D printing. *NPG Asia Mater*. 2018;10(4):82-9.
- 22 123. Huang J, Qin Q, Wang J. A Review of Stereolithography: Processes and
23 Systems. *Processes [Internet]*. 2020; 8(9).
- 24 124. Schmidleithner C, Kalaskar DM. *Stereolithography*. IntechOpen; 2018.
- 25 125. Nguyen KT, West JL. Photopolymerizable hydrogels for tissue engineering
26 applications. *Biomaterials*. 2002;23(22):4307-14.
- 27 126. Cooke MN, Fisher JP, Dean D, et al. Use of stereolithography to manufacture
28 critical-sized 3D biodegradable scaffolds for bone ingrowth. *J Biomed Mater Res B*
29 *Appl Biomater*. 2003;64B(2):65-9.
- 30 127. Harris RA, Newlyn HA, Hague RJM, et al. Part shrinkage anomalies from
31 stereolithography injection mould tooling. *Int J Mach Tools Manuf*. 2003;43(9):879-
32 87.
- 33 128. Wang WL, Cheah CM, Fuh JYH, et al. Influence of process parameters on
34 stereolithography part shrinkage. *Mater Des*. 1996;17(4):205-13.
- 35 129. Kim K, Yeatts A, Dean D, et al. Stereolithographic Bone Scaffold Design
36 Parameters: Osteogenic Differentiation and Signal Expression. *Tissue Eng Part B*
37 *Rev*. 2010;16(5):523-39.
- 38 130. Sinha RP, Häder D-P. UV-induced DNA damage and repair: a review.
39 *Photochem Photobiol Sci*. 2002;1(4):225-36.
- 40 131. de Gruijl FR, van Kranen HJ, Mullenders LHF. UV-induced DNA damage,
41 repair, mutations and oncogenic pathways in skin cancer. *Journal of Photochemistry*
42 *and Photobiology B: Biology*. 2001;63(1):19-27.
- 43 132. Palmero EM, Bollero A. 3D and 4D Printing of Functional and Smart
44 Composite Materials. In: Brabazon D, editor. *Encyclopedia of Materials: Composites*.
45 Oxford: Elsevier; 2021. p. 402-19.
- 46 133. Ahmad N, Gopinath P, Vinogradov A. 3D printing in medicine: Current
47 challenges and potential applications. *3D Printing Technology in*
48 *Nanomedicine*2019. p. 1-22.
- 49 134. Dávila J, Neto P, Noritomi P, et al. Hybrid manufacturing: a review of the
50 synergy between directed energy deposition and subtractive processes. *International*
51 *Journal of Advanced Manufacturing Technology*. 2020;110.

- 1 135. Ashish, Ahmad N, Gopinath P, et al. Chapter 1 - 3D Printing in Medicine:
2 Current Challenges and Potential Applications. In: Ahmad N, Gopinath P, Dutta R,
3 editors. 3D Printing Technology in Nanomedicine: Elsevier; 2019. p. 1-22.
- 4 136. Rouf S, Malik A, Singh N, et al. Additive manufacturing technologies: Industrial
5 and medical applications. *Sustainable Operations and Computers*. 2022;3.
- 6 137. Nadagouda MN, Ginn M, Rastogi V. A review of 3D printing techniques for
7 environmental applications. *Current Opinion in Chemical Engineering*. 2020;28:173-
8 8.
- 9 138. Gibson I, Rosen D, Stucker B. *Additive Manufacturing Technologies: 3D
10 Printing, Rapid Prototyping, and Direct Digital Manufacturing*: Springer New York;
11 2014.
- 12 139. He J, Xia P, Li D. Development of melt electrohydrodynamic 3D printing for
13 complex microscale poly (ϵ -caprolactone) scaffolds. *Biofabrication*.
14 2016;8(3):035008.
- 15 140. Hassanin H, Modica F, El-Sayed MA, et al. Manufacturing of Ti-6Al-4V Micro-
16 Implantable Parts Using Hybrid Selective Laser Melting and Micro-Electrical
17 Discharge Machining. *Advanced Engineering Materials*. 2016;18(9):1544-9.
- 18 141. Cheng K, Xiong W, Li Y, et al. In-situ deposition of three-dimensional
19 graphene on selective laser melted copper scaffolds for high performance
20 applications. *Composites Part A: Applied Science and Manufacturing*.
21 2020;135:105904.
- 22 142. Lam CXF, Mo XM, Teoh SH, et al. Scaffold development using 3D printing
23 with a starch-based polymer. *Mater Sci Eng C Mater Biol Appl*. 2002;20(1):49-56.
- 24 143. Zeltinger J, Sherwood JK, Graham DA, et al. Effect of Pore Size and Void
25 Fraction on Cellular Adhesion, Proliferation, and Matrix Deposition. *Tissue
26 Engineering*. 2001;7(5):557-72.
- 27 144. Therriault D, White SR, Lewis JA. Chaotic mixing in three-dimensional
28 microvascular networks fabricated by direct-write assembly. *Nat Mater*.
29 2003;2(4):265-71.
- 30 145. Do A-V, Smith R, Acri TM, et al. 9 - 3D printing technologies for 3D scaffold
31 engineering. In: Deng Y, Kuiper J, editors. *Functional 3D Tissue Engineering
32 Scaffolds*: Woodhead Publishing; 2018. p. 203-34.
- 33 146. Xiong Z, Yan Y, Wang S, et al. Fabrication of porous scaffolds for bone tissue
34 engineering via low-temperature deposition. *Scripta Materialia*. 2002;46(11):771-6.
- 35 147. Yan Y, Xiong Z, Hu Y, et al. Layered manufacturing of tissue engineering
36 scaffolds via multi-nozzle deposition. *Materials Letters*. 2003;57(18):2623-8.
- 37 148. Vozzi G, Previti A, De Rossi D, et al. Microsyringe-Based Deposition of Two-
38 Dimensional and Three-Dimensional Polymer Scaffolds with a Well-Defined
39 Geometry for Application to Tissue Engineering. *Tissue Engineering*. 2002;8(6):1089-
40 98.
- 41 149. Landers R, Mülhaupt R. Desktop manufacturing of complex objects,
42 prototypes and biomedical scaffolds by means of computer-assisted design
43 combined with computer-guided 3D plotting of polymers and reactive oligomers.
44 *Macromol Mater Eng*. 2000;282(1):17-21.
- 45 150. An J, Teoh JEM, Suntornnond R, et al. Design and 3D Printing of Scaffolds
46 and Tissues. *Engineering*. 2015;1(2):261-8.
- 47 151. Woodfield TBF, Malda J, de Wijn J, et al. Design of porous scaffolds for
48 cartilage tissue engineering using a three-dimensional fiber-deposition technique.
49 *Biomaterials*. 2004;25(18):4149-61.

- 1
2
3 1 152. Wang F, Shor L, Darling A, et al., editors. Precision Extruding Deposition and
4 2 Characterization of Cellular Poly-e-Caprolactone Tissue Scaffolds 573. 2003
5 3 International Solid Freeform Fabrication Symposium; 2003.
6 4 153. Tan KH, Chua CK, Leong KF, et al. Scaffold development using selective laser
7 5 sintering of polyetheretherketone–hydroxyapatite biocomposite blends. *Biomaterials*.
8 6 2003;24(18):3115-23.
9 7 154. Wang D, Wang Y, Wu S, et al. Customized a Ti6Al4V bone plate for complex
10 8 pelvic fracture by selective laser melting. *Materials*. 2017;10(1):35.
11 9 155. Turnbull G, Clarke J, Picard F, et al. 3D bioactive composite scaffolds for bone
12 10 tissue engineering. *Bioact Mater*. 2018;3(3):278-314.
13 11 156. Chu TMG, Halloran JW, Hollister SJ, et al. Hydroxyapatite implants with
14 12 designed internal architecture. *Journal of Materials Science: Materials in Medicine*.
15 13 2001;12(6):471-8.
16 14 157. Bittner SM, Guo JL, Melchiorri A, et al. Three-dimensional printing of
17 15 multilayered tissue engineering scaffolds. *Materials Today*. 2018;21(8):861-74.
18
19
20
21
22
23
24
25
26
27
28
29
30
31
32
33
34
35
36
37
38
39
40
41
42
43
44
45
46
47
48
49
50
51
52
53
54
55
56
57
58
59
60

1
2
3
4
5
6
7
8
9
10
11
12
13
14
15
16
17
18
19
20
21
22
23
24
25
26
27
28
29
30
31
32
33
34
35
36
37
38
39
40
41
42
43
44
45
46
47
48
49
50
51
52
53
54
55
56
57
58
59
60

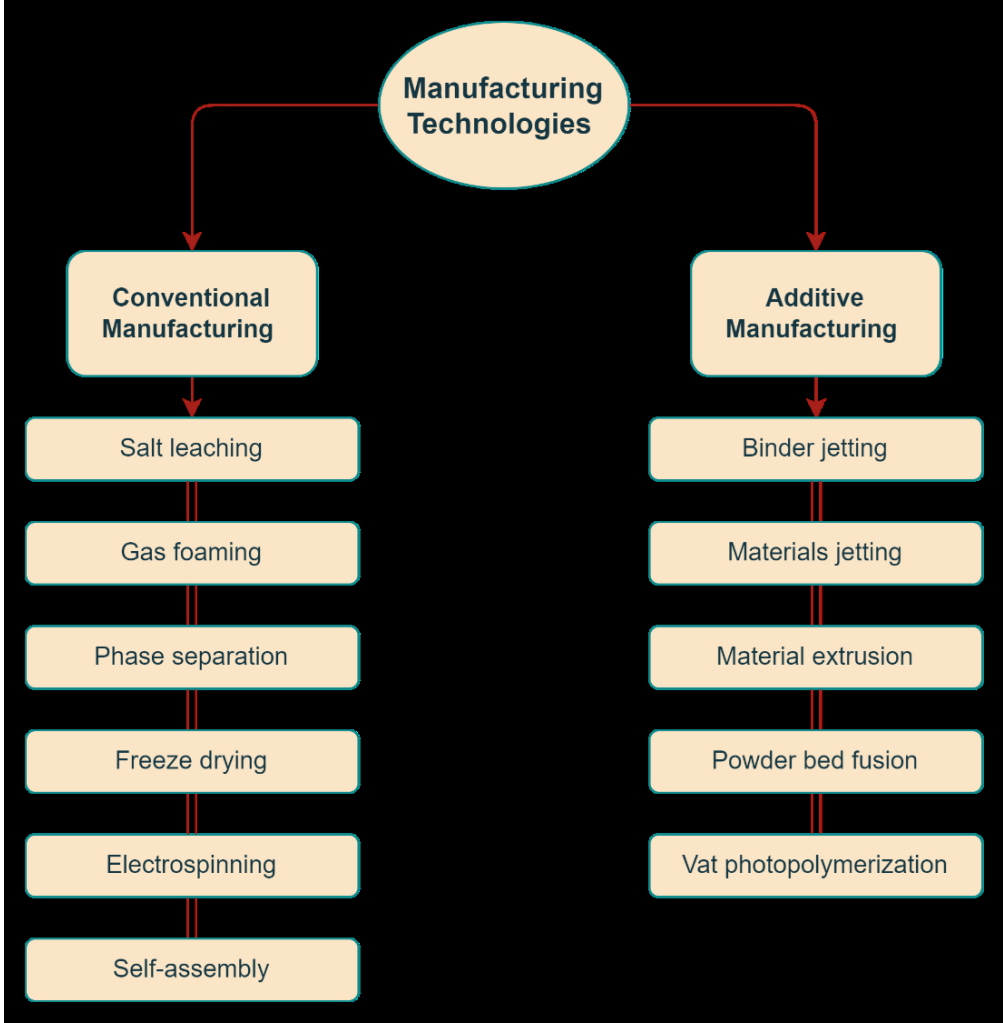


Figure 1. Flowchart of manufacturing technologies.

127x129mm (220 x 220 DPI)

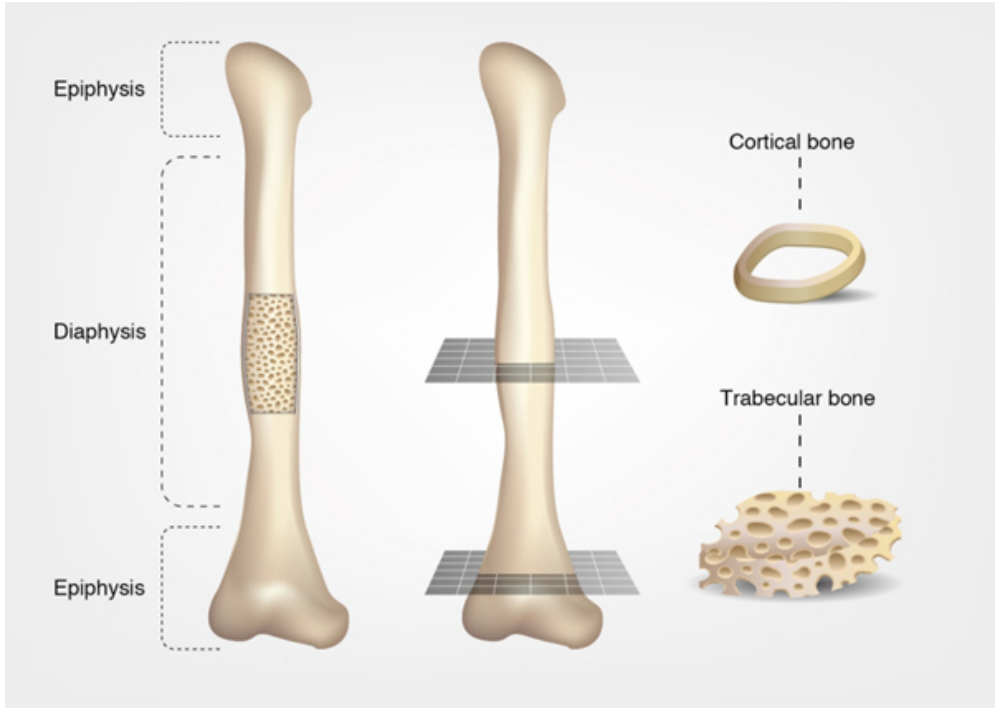


Figure 2. A long bone's macroscopic structure.

160x113mm (96 x 96 DPI)

1
2
3
4
5
6
7
8
9
10
11
12
13
14
15
16
17
18
19
20
21
22
23
24
25
26
27
28
29
30
31
32
33
34
35
36
37
38
39
40
41
42
43
44
45
46
47
48
49
50
51
52
53
54
55
56
57
58
59
60

1
2
3
4
5
6
7
8
9
10
11
12
13
14
15
16
17
18
19
20
21
22
23
24
25
26
27
28
29
30
31
32
33
34
35
36
37
38
39
40
41
42
43
44
45
46
47
48
49
50
51
52
53
54
55
56
57
58
59
60

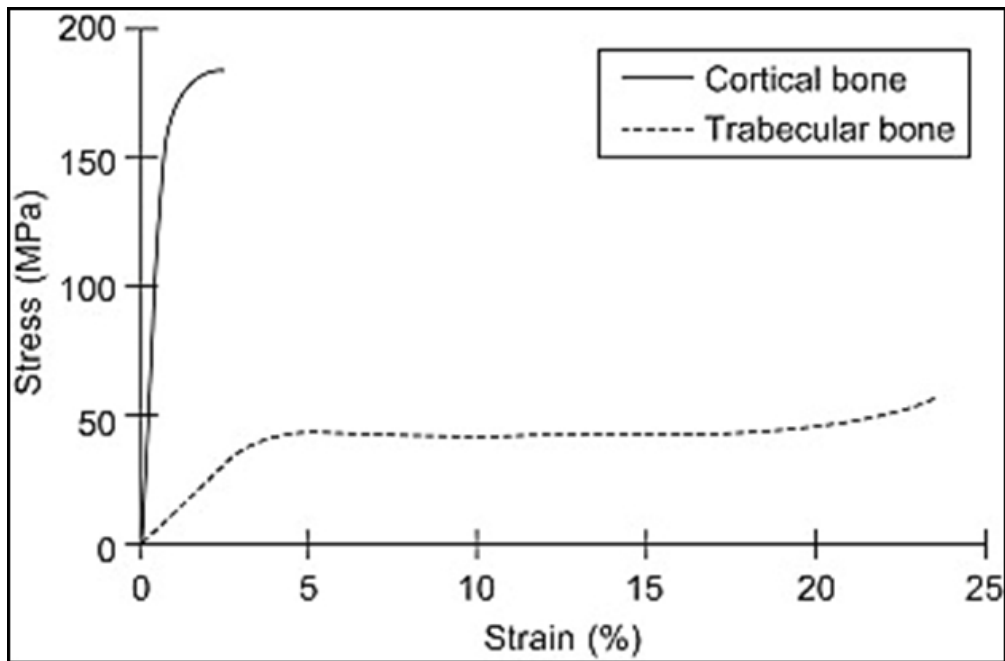


Figure 3. A comparison between the stress-strain properties of trabecular and cortical bones. Adapted from Damien Lacroix (21).

140x92mm (113 x 113 DPI)

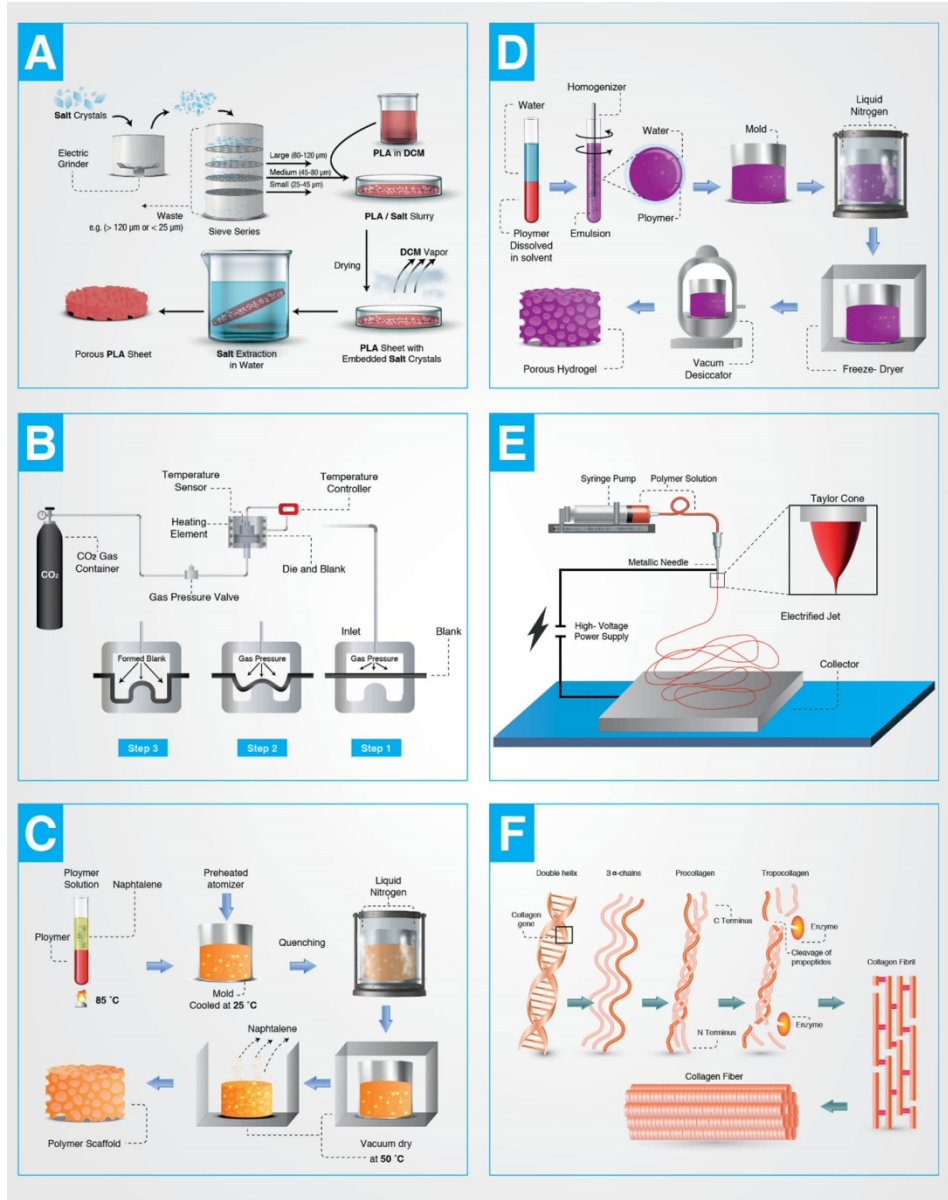


Figure 4. Conventional manufacturing techniques of bone scaffolds, (a) Salt leaching, (b) Gas forming, (c) Phase separation, (d) Freeze-drying, (e) Electrospinning and (f) Self-assembly.

169x213mm (220 x 220 DPI)

1
2
3
4
5
6
7
8
9
10
11
12
13
14
15
16
17
18
19
20
21
22
23
24
25
26
27
28
29
30
31
32
33
34
35
36
37
38
39
40
41
42
43
44
45
46
47
48
49
50
51
52
53
54
55
56
57
58
59
60

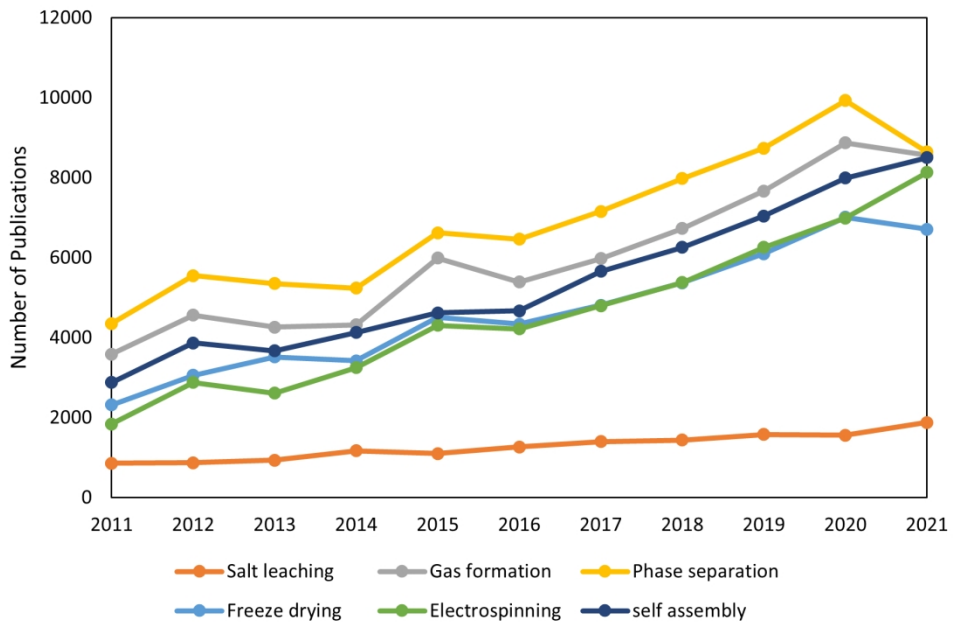


Figure 5. Number of papers published on bone scaffold fabricated by each conventional manufacturing technique over the last 10 years.

150x97mm (330 x 330 DPI)

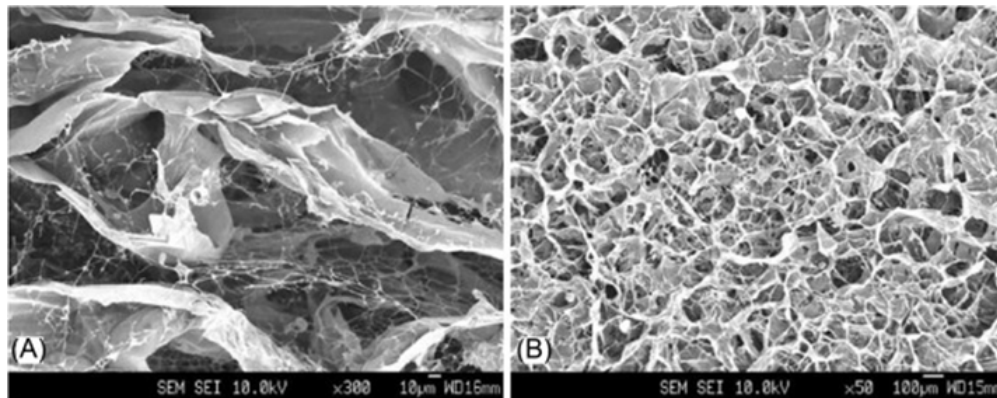


Figure 6. Collagen-coated chitin scaffold morphologies: (a) cross-section and (b) surface. Adopted from Sang Bong Lee (47).

160x63mm (113 x 113 DPI)

1
2
3
4
5
6
7
8
9
10
11
12
13
14
15
16
17
18
19
20
21
22
23
24
25
26
27
28
29
30
31
32
33
34
35
36
37
38
39
40
41
42
43
44
45
46
47
48
49
50
51
52
53
54
55
56
57
58
59
60

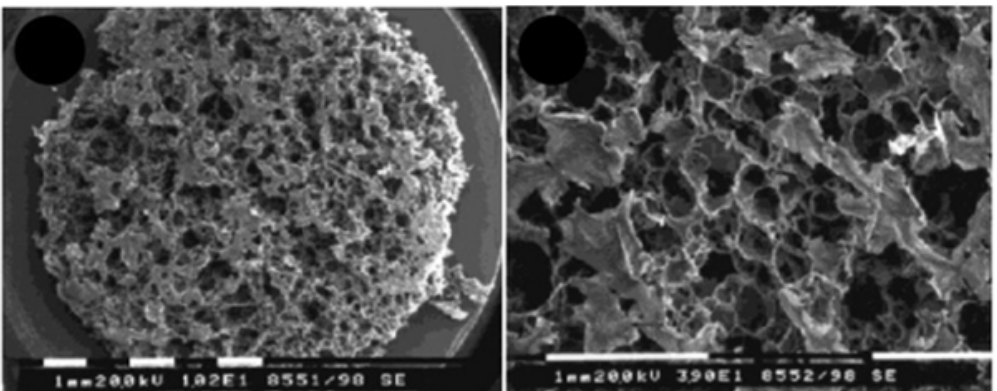
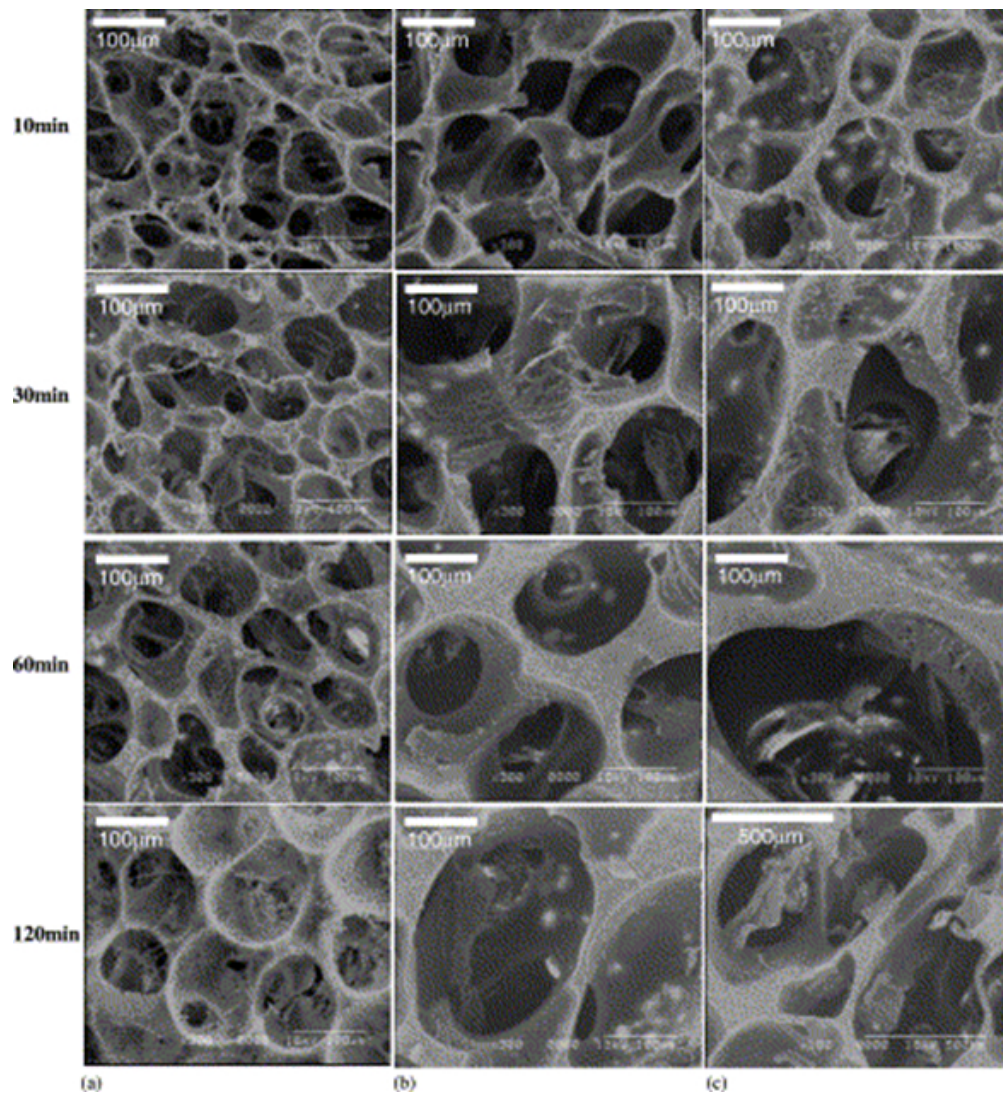


Figure 7. SEM images of surface morphology of PLLA scaffolds. Adopted from Nam (56).

159x64mm (96 x 96 DPI)



41
42
43
44
45
46
47
48
49
50
51
52
53
54
55
56
57
58
59
60

Figure 8. scanning electron micrograph of PLLA membranes as a function of aging time at quenching temperatures of 25°C (A), 30°C (B), and 35°C (C). Adopted from H Do Kim (62).

155x167mm (96 x 96 DPI)

1
2
3
4
5
6
7
8
9
10
11
12
13
14
15
16
17
18
19
20
21
22
23
24
25
26
27
28
29
30
31
32
33
34
35
36
37
38
39
40
41
42
43
44
45
46
47
48
49
50
51
52
53
54
55
56
57
58
59
60

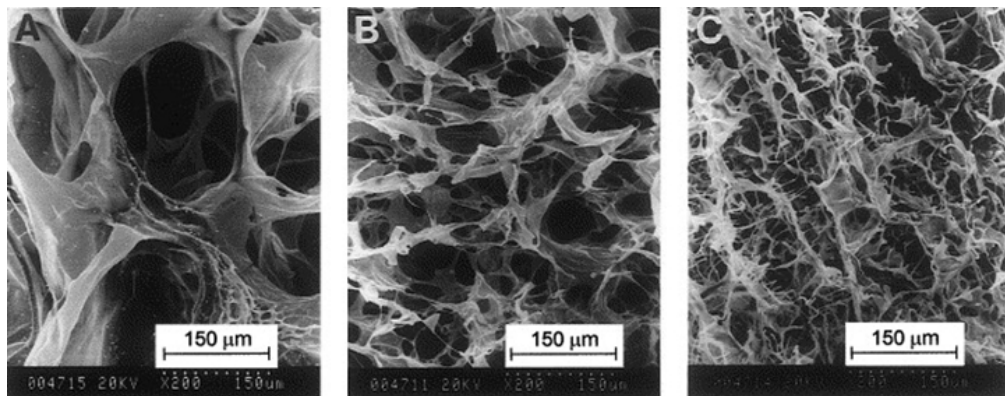


Figure 9. Effect of freezing temperature on morphology of the matrix. Collagen-hyaluronic acid scanning electron micrograph freeze dried at -20°C (A), -70°C (B) and -196°C (C) (magnification $\times 200$). Adopted from SN Park (66).

161x62mm (113 x 113 DPI)

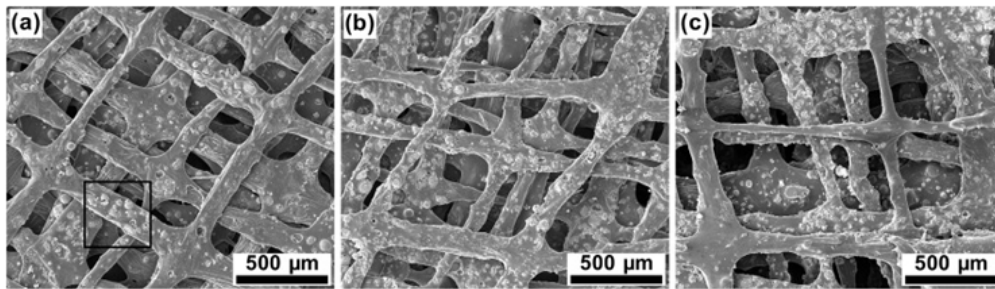


Figure 10. Morphological characterisation of the PCL/HA composite scaffolds. SEM image of (a) PCL/0.3 HA scaffold, (b) PCL/0.4 HA scaffold and (c) PCL/0.5 HA scaffold. Adopted from Feng-LiHe (72).

166x48mm (113 x 113 DPI)

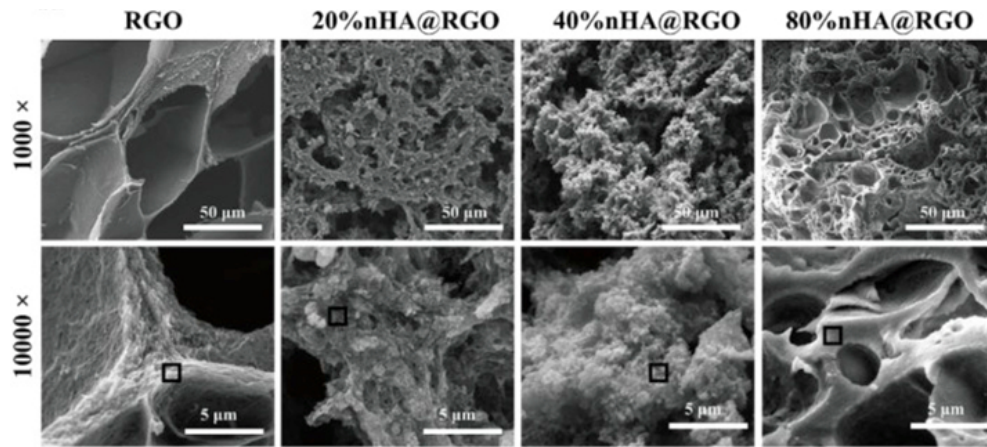


Figure 11. SEM of the nHA@RGO scaffold with the different nHA loading ratios. Reduced graphene oxide (RGO) and nano-hydroxyapatite (nHA). Adopted from WeiNie (77).

162x71mm (113 x 113 DPI)

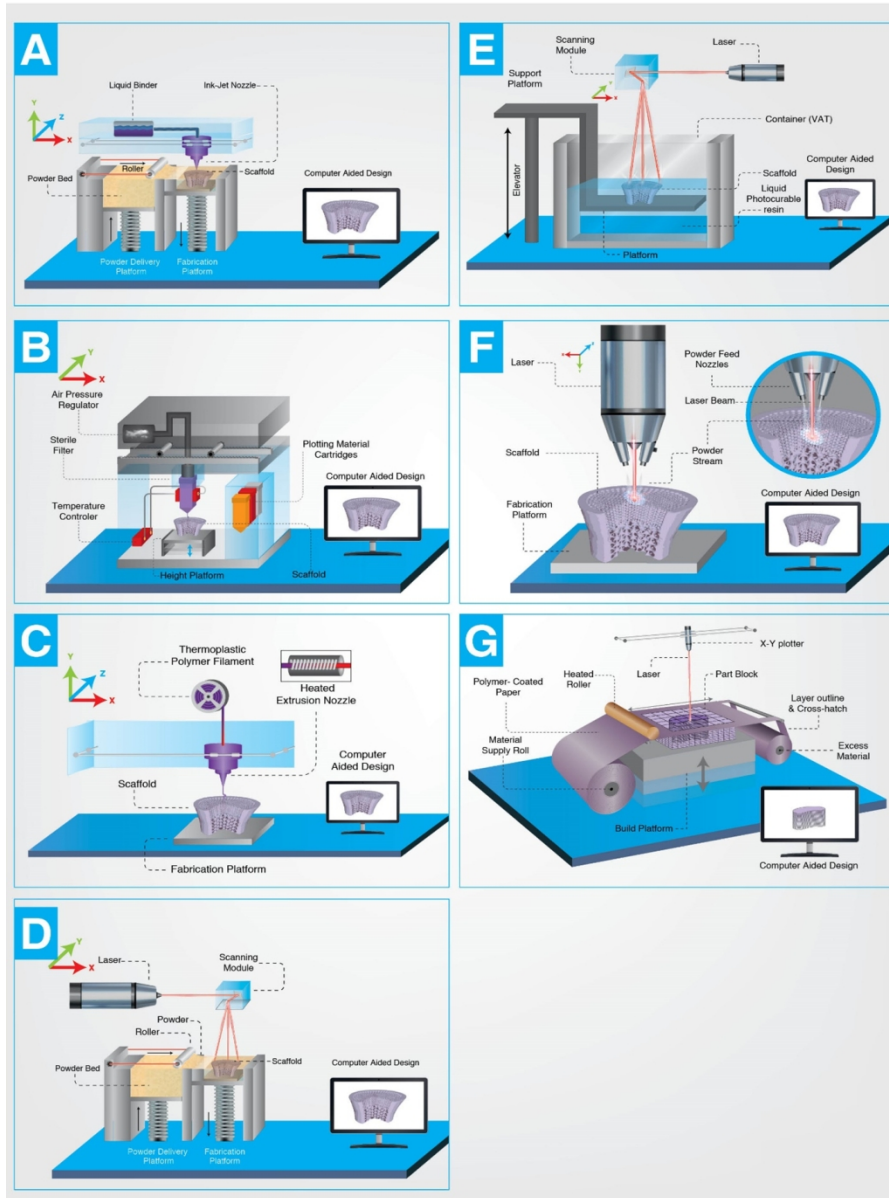


Figure 12. 3D printing techniques, (a) Binder jetting, (b) Materials jetting, (c) Materials extrusion, (d) Powder bed fusion, (e) Vat photopolymerisation, (f) Directed energy deposition, (g) Sheet lamination.

164x219mm (220 x 220 DPI)

1
2
3
4
5
6
7
8
9
10
11
12
13
14
15
16
17
18
19
20
21
22
23
24
25
26
27
28
29
30
31
32
33
34
35
36
37
38
39
40
41
42
43
44
45
46
47
48
49
50
51
52
53
54
55
56
57
58
59
60

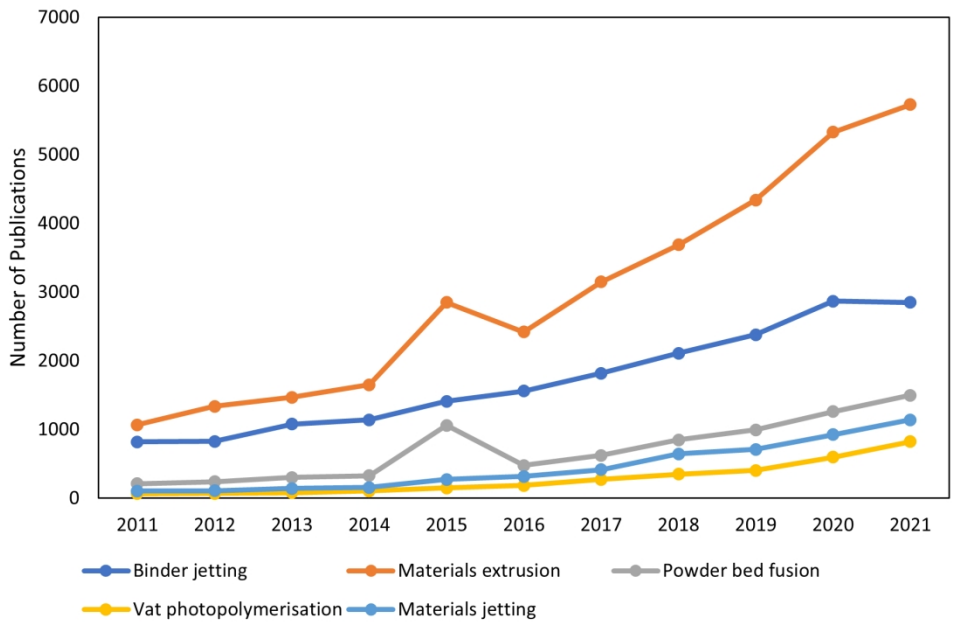


Figure 13. Number of papers published on bone scaffold fabricated by each 3D printing technique over the last 10 years.

153x99mm (330 x 330 DPI)

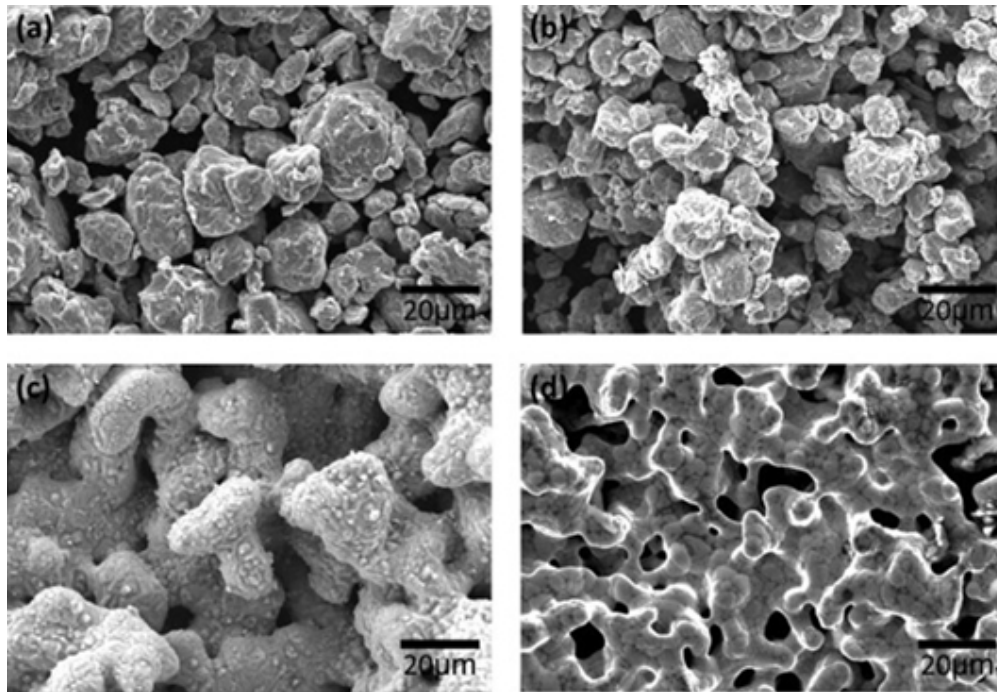


Figure 14. Morphology of (a) Fe-Mn powders (b) Fe-Mn-1Ca powders, (c) 3D printed Fe-Mn sample, and (d) 3D printed Fe-Mn-1Ca sample. Adopted from Hong D (93).

119x82mm (113 x 113 DPI)

1
2
3
4
5
6
7
8
9
10
11
12
13
14
15
16
17
18
19
20
21
22
23
24
25
26
27
28
29
30
31
32
33
34
35
36
37
38
39
40
41
42
43
44
45
46
47
48
49
50
51
52
53
54
55
56
57
58
59
60

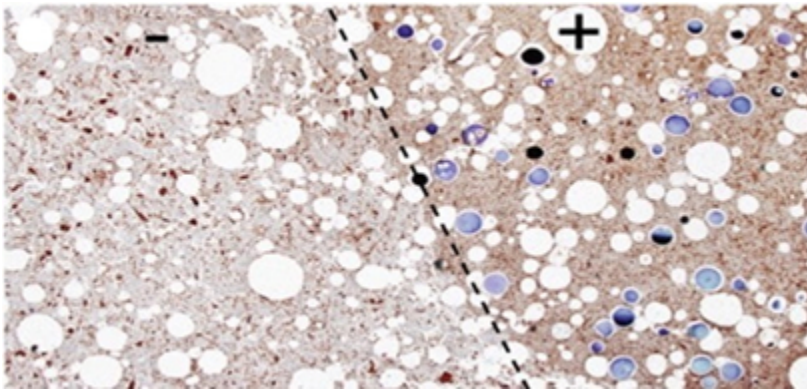


Figure 15. 3D printed matrigel-alginate scaffold the two regions (- without VEGF, + VEGF-laden GMPs).
Adopted from M. T. Poldervaart (97).

107x51mm (96 x 96 DPI)

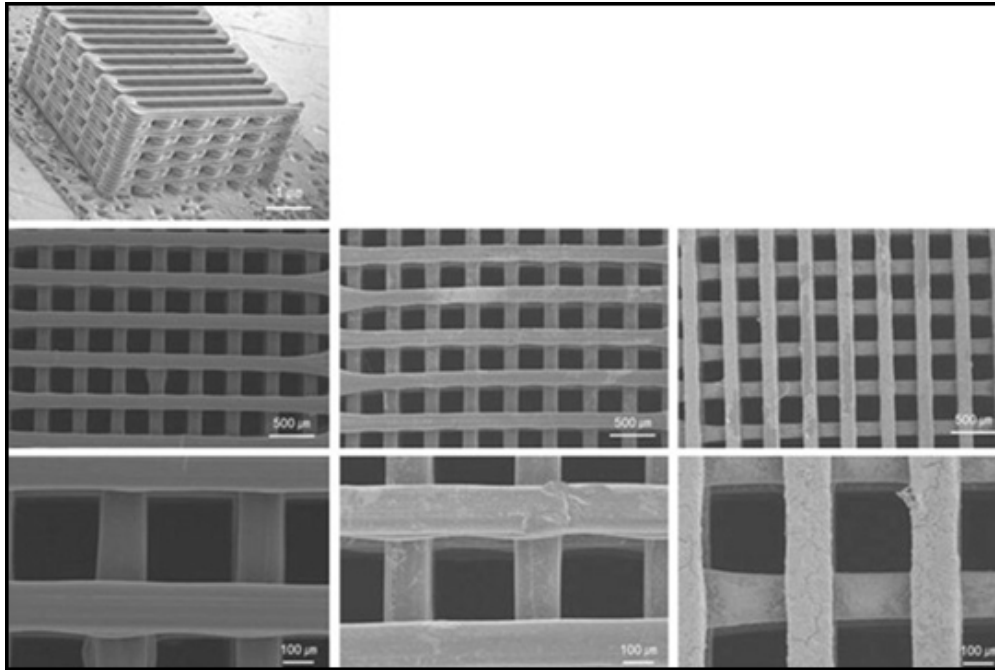


Figure 16. SFF-based 3-D PCL/PLGA scaffold. Adopted from J. M. Hong (105).

122x81mm (113 x 113 DPI)

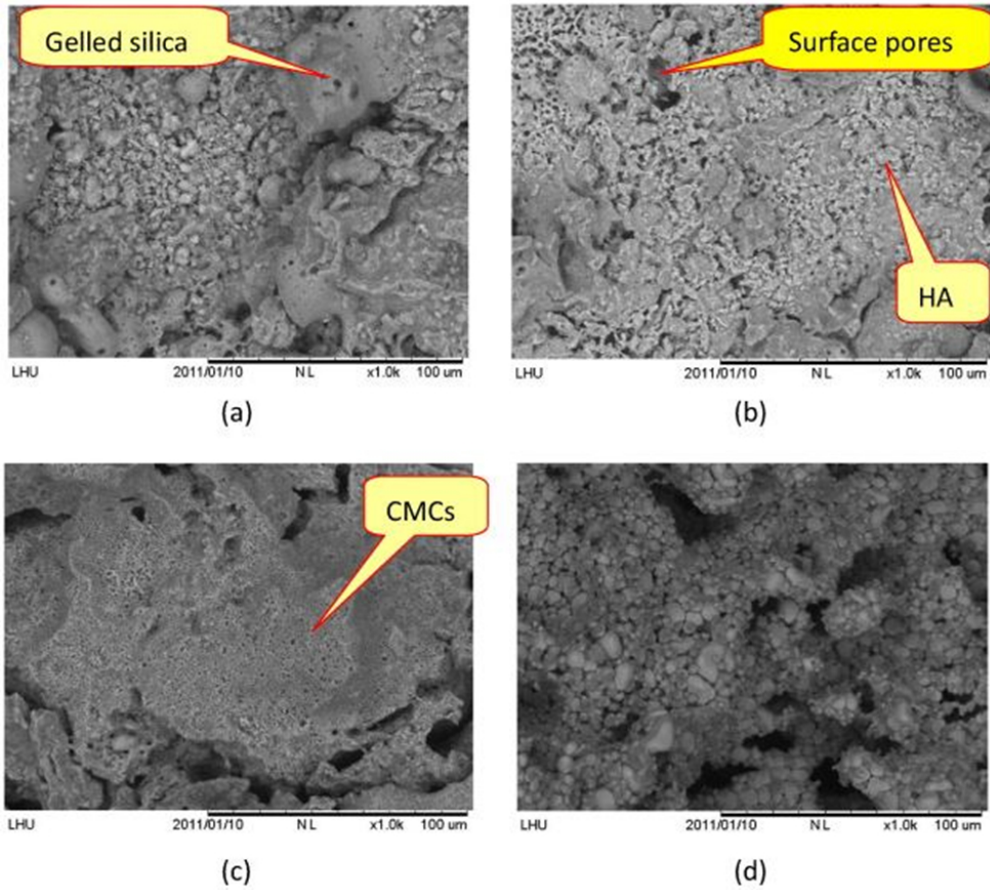


Figure 17. SEM images of the scaffold at (a) ambient temperature, (b) 1,200 °C, (c) 1,300 °C, and (d) 1,400 °C. hydroxyapatite (HA) and Ceramic-matrix composites (CMCs). Adopted from F.-H. Liu (117).

114x104mm (216 x 216 DPI)

1
2
3
4
5
6
7
8
9
10
11
12
13
14
15
16
17
18
19
20
21
22
23
24
25
26
27
28
29
30
31
32
33
34
35
36
37
38
39
40
41
42
43
44
45
46
47
48
49
50
51
52
53
54
55
56
57
58
59
60



Figure 18. fabricated scaffold using SLA. Adopted from M. N. Cooke (124).

113x84mm (100 x 100 DPI)

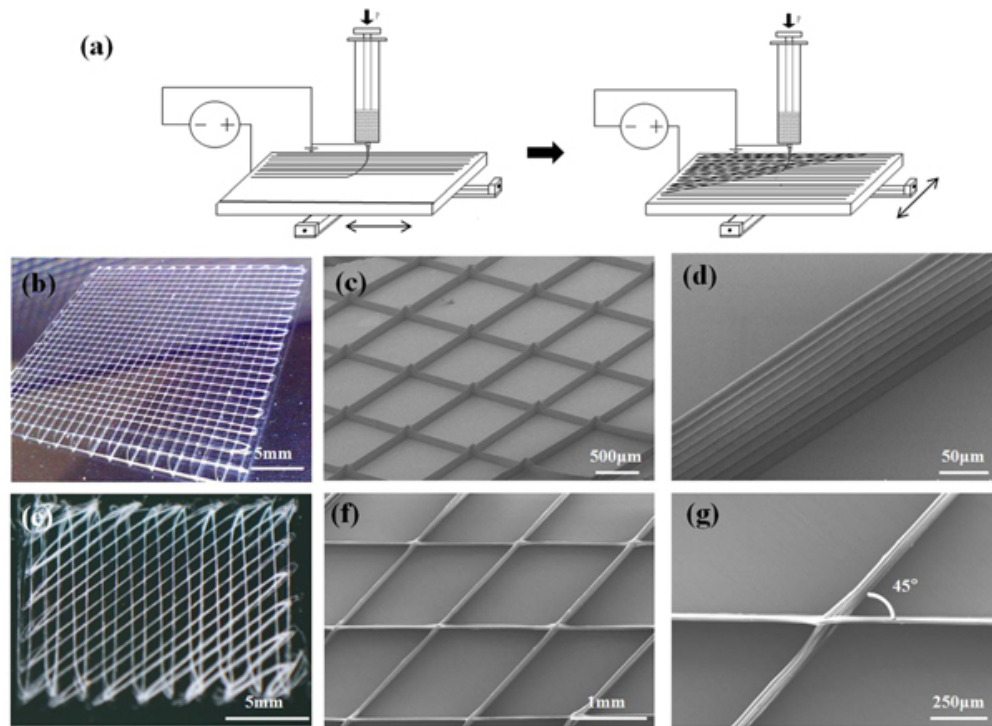


Figure 19. Fiber orientation manipulation during the melt electrohydrodynamic printing process. (a) Schematic illustration of manipulating fiber orientation through directing stage movement, (b-d) microscopic images of the printed scaffold, which have fibers spaced at 1 mm intervals and oriented at 90° and (e-g) oriented at 45°. Adopted from Jiankang He (139).

159x115mm (96 x 96 DPI)

1
2
3 **Figure 1.** Flowchart of manufacturing technologies.
4
5
6

7 **Figure 2.** A long bone's macroscopic structure.
8
9

10
11 **Figure 3.** A comparison between the stress-strain properties of trabecular and cortical bones.
12
13 Adapted from Damien Lacroix (21).
14
15

16
17 **Figure 4.** Conventional manufacturing techniques of bone scaffolds, (a) Salt leaching, (b) Gas
18 forming, (c) Phase separation, (d) Freeze-drying, (e) Electrospinning and (f) Self-assembly.
19
20
21

22
23 **Figure 5.** Number of papers published on bone scaffold fabricated by each conventional
24 manufacturing technique over the last 10 years.
25
26
27

28
29 **Figure 6.** Collagen-coated chitin scaffold morphologies: (a) cross-section and (b) surface.
30
31 Adopted from Sang Bong Lee (47).
32
33

34
35 **Figure 7.** SEM images of surface morphology of PLLA scaffolds. Adopted from Nam (56).
36
37
38

39
40 **Figure 8.** scanning electron micrograph of PLLA membranes as a function of aging time at
41 quenching temperatures of 25°C (A), 30°C (B), and 35°C (C). Adopted from H Do Kim (62).
42
43
44

45
46 **Figure 9.** Effect of freezing temperature on morphology of the matrix. Collagen-hyaluronic
47 acid scanning electron micrograph freeze-dried at -20 ° C (A), -70 ° C (B) and -196 ° C (C)
48 (magnification ×200). Adopted from SN Park (66).
49
50
51

52
53 **Figure 10.** Morphological characterisation of the PCL/HA composite scaffolds. SEM image
54 of (a) PCL/0.3 HA scaffold, (b) PCL/0.4 HA scaffold and (c) PCL/0.5 HA scaffold. Adopted
55 from Feng-LiHe (72).
56
57
58
59
60

1
2
3 **Figure 11.** SEM of the nHA@RGO scaffold with the different nHA loading ratios. Reduced
4 graphene oxide (RGO) and nano-hydroxyapatite (nHA). Adopted from WeiNie (77).
5
6
7
8

9 **Figure 12.** 3D printing techniques, (a) Binder jetting, (b) Materials jetting, (c) Materials
10 extrusion, (d) Powder bed fusion, (e) Vat photopolymerisation, (f) Directed energy deposition,
11 (g) Sheet lamination.
12
13
14

15
16
17 **Figure 13.** Number of papers published on bone scaffold fabricated by each 3D printing
18 technique over the last 10 years.
19
20
21
22

23 **Figure 14.** Morphology of (a) Fe-Mn powders (b) Fe-Mn-1Ca powders, (c) 3D printed Fe-Mn
24 sample, and (d) 3D printed Fe-Mn-1Ca sample. Adopted from Hong D (93).
25
26
27
28

29 **Figure 15.** 3D printed matrigel-alginate scaffold the two regions (– without VEGF, + VEGF-
30 laden GMPs). Adopted from M. T. Poldervaart (97).
31
32
33
34

35 **Figure 16.** SFF-based 3-D PCL/PLGA scaffold. Adopted from J. M. Hong (105).
36
37
38

39 **Figure 17.** SEM images of the scaffold at (a) ambient temperature, (b) 1,200 °C, (c) 1,300 °C,
40 and (d) 1,400 °C. hydroxyapatite (HA) and Ceramic-matrix composites (CMCs). Adopted
41 from F.-H. Liu (117).
42
43
44
45

46
47 **Figure 18.** fabricated scaffold using SLA. Adopted from M. N. Cooke (124).
48
49
50

51 **Figure 19.** Fiber orientation manipulation during the melt electrohydrodynamic printing
52 process. (a) Schematic illustration of manipulating fiber orientation through directing stage
53 movement, (b-d) microscopic images of the printed scaffold, which have fibers spaced at 1 mm
54 intervals and oriented at 90° and (e-g) oriented at 45°. Adopted from Jiankang He (139).
55
56
57
58
59
60

Table 1. Terms, definitions and examples of bone repair [40].

Term	Definition	Example
Osteogenesis	The process by which new bone is synthesised using donor cells taken either from the host or the graft donor.	Stem cell, autografts transplants
Osteoconduction	The passive ingrowth of host vasculature, tissue, and cells into an implanted scaffold.	Phosphate cements or calcium sulphate resorption
Osteoinduction	Exogenous growth factors enable host mesenchymal stem cells (MSCs) to differentiate into osteoblasts and chondroblasts capable of producing new bone.	Proteins involved in bone morphogenesis

Table 2. Morphological properties of collagen-HA membranes. Adopted from SN Park [66].

Freezing temperature	Porosity (%)		Pore size (μm)	
	Before crosslinking	After crosslinking	Before crosslinking	After crosslinking
-196°C	58.1 \pm 3.4	61.95 \pm 3.8	40 \pm 7	84 \pm 20
-70°C	59.28 \pm 4.9	62.3 \pm 4.8	90 \pm 16	186 \pm 29
-20°C	66.46 \pm 2.6	64.93 \pm 2.3	230 \pm 52	190 \pm 42

Table 3. summary of conventional manufacturing.

Manufacturing technique	Main applications	Advantages	Disadvantages	Ref.
Salt leaching	Forming porosity in part by employing salt particles	<ul style="list-style-type: none"> Controlled pore size Suitable for manufacturing of membranes 	<ul style="list-style-type: none"> Lack of pores distribution control Lack of scaffold shape control 	[43, 48] [50]

Gas foaming	Forming porosity in part by applying high pressure	<ul style="list-style-type: none"> • It does not use chemical solvents • It is capable of fabricating parts with very high porosity 	<ul style="list-style-type: none"> • Pore sizes are difficult to control • It employs a high temperature • Lack of scaffold shape control 	[57, 58] [59]
Phase separation	Forming porosity in part by employing chemical solvents	<ul style="list-style-type: none"> • It does not require post-processing 	<ul style="list-style-type: none"> • Pore sizes are very small • Lack of scaffold shape control 	[43, 59]
Freeze-drying	Forming porosity in part by freezing the liquid mixture	<ul style="list-style-type: none"> • Pore sizes can be adjusted by controlling the temperatures 	<ul style="list-style-type: none"> • Lack of scaffold shape control • high energy consumption • uses cytotoxic solvents 	[67, 68] [66]
Electrospinning	Forming solid nano size fibres	<ul style="list-style-type: none"> • Mechanical and porosity properties of the fibre can be controlled by regulating the voltage and distance 	<ul style="list-style-type: none"> • Lack of scaffold shape control 	[73, 74] [72]
Self-assembly	Forming a pattern by the interactions of two components without external direction	<ul style="list-style-type: none"> • It does not require the use of cytotoxic solvents 	<ul style="list-style-type: none"> • Pore sizes are very small • It necessitates greater attention to molecular design and intricate synthesis 	[76] [77]

Table 4. summary of the 3D printing techniques.

AM technology	Resolution (μm)	Material	Strength	Weakness	Refs
Binder jetting	200-300	PLGA, PLLA, PEEK-HA, PCL, starch-based polymer	<ul style="list-style-type: none"> No support structure is required Fast processing Uses a variety of materials 	<ul style="list-style-type: none"> Can require post-processing Powdery surface finish Trapped powder 	[142, 143]
Materials jetting	10-1000	PCL, PLLA, TCP, Hydrogel, Organic ink	<ul style="list-style-type: none"> Uses an enhanced range of materials Can incorporate biomolecule 	<ul style="list-style-type: none"> Low mechanical strength Smooth surface Low accuracy Slow processing Complex design requires support structure 	[144-149]
Materials extrusion	250	PCL, PP-TCP, PCL-HA, PCL-TCP, PETG-PBT, PLLA-TCP, PLA	<ul style="list-style-type: none"> Good mechanical strength Preparation time is reduced 	<ul style="list-style-type: none"> High temperature Need to produce filament material Narrow processing window Complex design can require support structure 	[108, 150-152]
Powder bed fusion	500	PEEK-HA, PCL, titanium, Stainless steel, cobalt-chromium alloys	<ul style="list-style-type: none"> Microporosity induced in the scaffold Uses an enhanced range of materials No support structure needed Fast processing 	<ul style="list-style-type: none"> Material must be in powder form High temperature Powdery surface finish Trapped powder Thermal damage can occur during processing 	[153-155]
Vat photopolymerisation	366	Resin, PPF, polyethylene glycol acrylate, HA	<ul style="list-style-type: none"> Control of both external and internal morphology Uses an enhanced range of materials High accuracy Fast processing 	<ul style="list-style-type: none"> Multistep involved Poor mechanical strength Damages cell during photo curing UV blue light can be toxic to cells 	[156, 157]

Poly(lactic-co-glycolic acid) (PLGA), Poly(L-lactide) (PLLA), (polyetheretherketone) (PEEK), Hydroxyapatite (HA), Polycaprolactone (PCL), Tricalcium phosphate (TCP), Polypropylene (PP), Polyethylene terephthalate glycol (PETG), Polybutylene terephthalate (PBT) and Paint protection film (PPF).